Received: 31 July 2022 | Revised: 15 October 2022 | Accepted: 28 November 2022

DOI: 10.1002/tal.1997

RESEARCH ARTICLE

WILEY

Special braced stairs versus typical braced frames. New architectural-structural-seismic approach to stair design

Carlos Montalbán Turon[1,2] | Yeudy F. Vargas Alzate[1]

[1]Department of Civil & Env. Eng. (DECA), Polytechnic University of Catalonia, Tech, Barcelona, 08034, Spain

[2]Department of Architectural Technology, Polytechnic University of Catalonia, Tech, Barcelona, 08028, Spain

Correspondence
Carlos Montalbán Turon, Department of Civil & Environmental Engineering (DECA), Polytechnic University of Catalonia, Barcelona Tech., 08034 Spain.
Email: carlos.montalban@upc.edu; cmtarqt@gmail.com

Summary

This paper presents a new approach to the project of steel buildings, mainly focused on the architectural, structural, and seismic design of stairs. The objective is to design a structural stair system capable of controlling seismic damage and contributing to the bracing system of the building. The article begins with a review of the seismic standard (ATC, FEMA, and EC8) on which the current design criteria for new buildings with stairs are based. The research is based on two spatial building models (A–B) with the same bracing elements but placed differently. Reference Model A follows classical design approaches. It means, stairs are considered nonstructural elements that do not influence the seismic behavior of the building. This structure corresponds to typical braced frames (IV-CBF and EBF) according to EC8. Model B includes a stair system designed to help control the effects of inter-story drifts and inertia forces. In this case, the same bracing elements of Model A were integrated into the stair structure of Model B. A comparative seismic behavior analysis of typically braced frames (A) versus specially braced stairs (B) is presented. The research was based on the static nonlinear (pushover) analysis and the capacity spectrum method (ATC-40) according to the seismic performance levels (FEMA) and damage limitation (EC8). Finally, the braced stairs was verified via nonlinear time-history analysis in order to better capture the structural safety of the evacuation routes and their influence on the behavior of the building. This deterministic analysis of the braced stairs verified satisfactory results compared to reference bracing systems.

KEYWORDS
architecture, bracing system, Eurocode 8, seismic behavior, steel building, structural stairs

1 | INTRODUCTION

The integrity of the staircase is essential to ensure rapid evacuation and assistance to building users. However, the need to escape from buildings may be impeded by the danger of the collapse of stairways in the event of a seismic emergency. The structural fragility of stairways under the effects of earthquakes can lead to loss of life, serious accidents, and costly property damage. Different safety codes (e.g., fire prevention) control the design of new buildings to ensure that stairways are the safest evacuation route in accidental situations.[1] Notwithstanding, the typical recommendation (in the event of a seismic emergency) for public building users is to avoid stairways.[2] The typical collapse of stairs has been studied in several articles, based on the inspection of buildings affected by earthquakes.[3] Subsequent studies have recognized the importance of stairs

on the seismic behavior of buildings.[4–6] Other research based on laboratory tests with full-scale steel structures on shaking tables warns that current stairways are sensitive to lateral displacements and highly susceptible to damage or collapse when subjected to earthquakes.[7,8] Recent articles confirm the need to improve the structural safety of stairs[9] and investigate new solutions.[10] Some articles have presented comparative studies of the structural behavior of reinforced concrete (RC) buildings with or without considering stairs in the analysis.[4,11–13] Recent research also for RC buildings propose solutions to isolate the stairs.[14–16] In spite of the above, the seismic design of buildings is generally based on idealized models without stairs, assuming that they are isolated from the main structure. This research verified that isolated stairs waste their potential as part of the lateral force-resisting system in steel buildings. Therefore, the motivation is to improve the structural safety of stairs in steel buildings by designing them as primary elements. The objective is to prevent damage on both the stairs and the main structure by utilizing dissipative elements. Since the feasibility of the novel braced stair system has been verified on simplified models, this research can be considered a pilot study.

2 | SEISMIC STANDARD REVIEW

This section (summarized in Table A1) provides an overview of the main seismic standards (ATC, FEMA, and EC8) on which the current design criteria for new buildings with stairs are based.

2.1 | Stairs, primary or secondary elements? (ATC-40)

ATC-40[17] incorporated the concept of "primary" and "secondary" elements. Primary elements are those required as part of the structural system to resist lateral loads. All other elements are designated as secondary elements. For a given level of performance, secondary elements are generally allowed to suffer more damage than primary elements. This standard considers that the degradation of secondary elements should not have significant effects on the lateral resistance capacity of the building. However, it is recommended not to design as secondary an excessive number of elements that are effective in resisting lateral forces. ATC-40 cautions that stairs can significantly modify the stiffness and strength of the frames and should not be overlooked. It also warns that stairs can act as diagonals to horizontal actions *(9.3.1 Building Model, ATC-40)*.

2.2 | Seismic performance levels in stairs (FEMA 356)

In *Chapter 2: General Requirements* of FEMA 356,[18] the designer is encouraged to include all elements with significant lateral stiffness into an analytical model that properly captures the deformation capacity under realistic inter-story drifts ratios (IDR). Nonetheless, certain elements may be determined not to be considered part of the lateral force-resisting system (if deformation compatibility checks are performed on these elements to ensure their adequacy). Specific evaluation requirements for stairs are defined in *Chapter 11.9 Architectural Components: Definition, Performance, and Acceptance Criteria (C11.9.8.2)*. Accordingly, stairs may be independent or integral to the main structure. If integral, they should be part of the structural analysis, with particular attention to the possibility of modification of the overall response due to localized stiffness. If the stairs are assumed to be isolated, their ability to withstand normal loads, direct acceleration, and loads transmitted through connections should also be verified. Hence, stairs may take the form of structural reinforcement or connection details to eliminate or reduce the interaction with the building structure. Acceptance criteria shall be applied to the stair structure to resist seismic design forces and tolerate expected relative displacements. The evaluation requirements of FEMA 356 state that the materials, condition of the stair members, and their connections to supports shall be considered in the evaluation *(C11.9.8.4)*. This standard defined the seismic performance levels, according to the force/deformation ratio in the plastic hinges of structural members. *Table C1-5 Nonstructural Performance Levels and Damage* states that emergency stairs should be usable at Life Safety (LS) level. The seismic performance level of Collapse Prevention (CP) poses a significant risk compared to LS due to the failure of nonstructural elements ("loss of use of stairs"). Note that when the structure is subjected to the maximum lateral force, it should not exceed the CP level.

2.3 | Damage limitation in stairs (EC8)

2.3.1 | Primary and secondary members (4.2.2, EC8)

The classification of building elements defined in EC8,[19] section *4.2.2 Primary and secondary seismic members*, establishes that a certain number of structural members may be designated as "secondary" seismic members, which are not part of the seismic action resistance

system of the building. The strength and stiffness of these elements against seismic actions is not considered. But it is specified that these members and their connections shall be designed and detailed to withstand gravity loads when subjected to displacements caused by the most unfavorable seismic condition. If stairs are considered part of the lateral force-resisting system, they must be modeled, designed, and detailed for earthquake resistance. Note that if stairs are not considered a primary seismic element, two checks should be carried out:

a. Lateral stiffness contribution of secondary members should not exceed 15% of primary *(4.2.2* [4], *EC8)*.
b. Designation of some structural elements as secondary seismic members should not change the classification of the structure from non-regular to regular *(4.2.2* [5], *EC8)*.

2.3.2 | Nonstructural elements (4.3.5, EC8)

The collapse of stairways poses a danger to users of buildings under seismic hazards. If considering stairs as a secondary element, the provisions of section *4.3.5 Nonstructural elements* should be applied:

a. Nonstructural elements that may cause risks to people, affect the main structure, or collapse should be verified under the seismic design action *(4.3.5.1* [1], *EC8)*.
b. For nonstructural elements of great importance or particularly dangerous nature, the seismic analysis shall be based on a realistic model of the structure. The analysis shall be based on an adequate response spectrum derived from the response of the supporting structural elements of the seismic-resistant system *(4.3.5.1* [2], *EC8)*.

To consider the stair structure as a nonstructural element, section *4.3.5.2 Verification* must be considered. This section establishes that nonstructural elements, their connections, and anchorages must be verified for the seismic design situation. Consideration should be given to the local transmission of actions by the attachment of the nonstructural elements and their influence on the seismic behavior of the overall structure.

2.3.3 | Damage limitation (4.4.3.2, EC8)

The main problem affecting the structural safety of stairs is the inter-story drift ratio (IDR) caused by lateral seismic loads. The damage limitation defined in EC8 has been applied according to section *4.4.3.2 Limitation of inter-storey drift*:

a. Buildings having nonstructural elements of brittle materials attached to the structure:

$$d_r \nu \leq 0{,}005\, h \tag{1}$$

b. Buildings having ductile nonstructural elements:

$$d_r \nu \leq 0{,}0075\, h \tag{2}$$

c. Buildings without nonstructural elements:

$$d_r \nu \leq 0{,}010\, h \tag{3}$$

where d_r is the design *IDR*, h is the floor height, and v is a reduction factor (the *IDR* considered in this research is option *b*).

2.4 | Project of new buildings with stairs (FEMA P-750)

Part 1. Provisions of FEMA P-750[20] also addresses the problem of the fragility of nonstructural elements and stairs under the effects of the earthquake: "Falling nonstructural components also cause deaths and injuries. Anchorage and bracing requirements for nonstructural components minimize this risk. These anchorages and bracing of nonstructural systems, along with reasonable limitations on differential movement between floors also serve to control the damage. The more restrictive IDR limitation can further reduce damage to elements connected to more than one floor."

2.5 | Reducing the risks of stairs (FEMA E-74)

FEMA E-74[21] also refers to the problem of seismic vulnerability of stairs (*6.3.8. Stairways*). This includes stairs between floors, which may be independent of the structure or integral to it. ASCE/SEI 7-10[22] provisions are cited as the building code. Systems required for life-safety purposes after an earthquake (e.g., stairways) must be designed to accommodate story drift while having sufficient strength to resist inertial loads. The minimum lateral loads, seismic relative displacement on stairways, and allowable story drifts are defined in ASCE/SEI 7-10. The retrofit standard provisions defined in ASCE/SEI 41-06[23] classify stairs as either acceleration or deformation sensitive, depending on predominant behavior. Components of stairs that are attached to frames or adjacent floors are considered deformation sensitive. All other components are considered acceleration sensitive. Note that damage is observed more often in concrete stairs because of their very rigid connections (not detailed for displacements). As commented above, the typical causes of damage in stairs are caused primarily by inter-story drifts, so it is more likely to occur in flexible buildings with larger inter-story drifts that in stiffer buildings. The acceptance criteria focus on verifying that stairs have sufficient strength to resist out-of-plane forces and can accommodate the expected relative displacements. When stairs are rigidly attached to both floors, their components act like diagonals. Thus, typical steel stairways can suffer dangerous damage if not specifically detailed for slip or provided with ductile connection details. Single-run steel stairs without slip connections can cause buckling or connection failures in stringers. However, if stairs have sliding connections but the designed differential displacement is exceeded, the structure of stairs may collapse.

3 | DEFINITION OF ANALYSIS MODELS

3.1 | Archetype building versus analysis model

Previous studies on the irregular or eccentric configuration of stairs in buildings detected alterations in the seismic behavior of the structure, such as global torsional effects and brittle collapse of stairs.[24] Figure 1a shows an archetype configured according to a seismic standard, in terms of regularity and symmetry. This type of stair provides the requirement of regularity and mechanical symmetry (plan and elevation). The *Singapore Civil Defense Force Code* [25] recommends scissor-type stairs for fire safety reasons. Figure 1b shows the floor plan of the reduced analysis model to simplify the calculation. The YZ braced frames of the reduced model are located on the B and E axes (12 m apart). However, in the archetype building, the braced frames are located on the B and J axes (32 m apart). The high torsional inertia of the archetype (according to *4.2.1.4, EC8*) allows assuming that it is not significantly affected by torsional modes. Since the specific global torsional characteristics of the reduced model should not affect the modal response of the archetype buildings, the rotational modes can be neglected in the analysis.

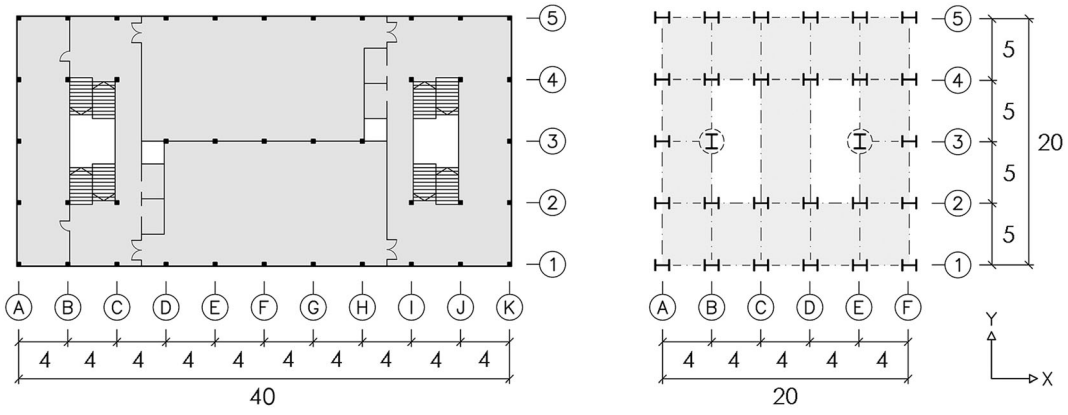

(a) *Archetype building (40x20 m²)* **(b)** *Reduced analysis model (20x20 m²)*

FIGURE 1 Floor plan of the archetype building versus the reduced analysis model

Figure 2 shows the typical braced frames (Model A) and the special braced stairs (Model B) designed as part of the lateral force-resisting system of the building. Model A shows the inverted-V concentrically braced frames (IV-CBF/green) and the eccentrically braced frame with a vertical shear link (EBF/red). As shown, the stairs and the inverted-V diagonals are incompatible in the same vertical core. But this architectural issue caused by building diagonals can be solved by relocating them to the stairs structure. Integrating the concentric diagonals into the stairs structure also can improve their seismic behavior. As shown in Model B, the new position of the concentric diagonals (green) braces the stair landing and the XZ frames. Part of the eccentric diagonals of Model A (red) can be used as stair stringers (blue). The reduced eccentric diagonals rigidly connected to the vertical shear link (red) brace the stair structure and the YZ frames, in the Y-direction.

Figure 3 shows the YZ elevation of the stair structure. This geometry complies with the general design rules for earthquake-resistant buildings (regularity and symmetry) applied to the stair local structure. The stair landing at mid-height (1.75 m) between floors (3.5 m) ensures the rigid diaphragm effect in its plane, becoming a key element of the bracing system. The fire safety standard requires that the width of each stair landing (2 m) should not be less than the width of the stairway (2 m). The stairs members are concentric to XZ frames but eccentric to the YZ beam (10 m). The slope of the stairs stringers is 30°. Rungs (30 x 17.5 cm) are modeled as steel beams (UPE 300). All stair stringers are defined with pinned end connections.

3.2 | Geometry of reduced Models A–B

Figure 4 shows a 3D view of the four-story analytical model (the main structural elements that are common to both analysis Models A–B). Figure 5a shows the YZ typical frame of Model B. Figure 5b shows the joint releases and cross-section sizes of the steel beams. Table 1 summarizes the dimensions of the reduced model. The XZ frames define five 4-m wide bays (20 m in total). The YZ frames define four 5-m wide bays (20 m in total). Table 2 presents the cross-section size of steel columns and beams in Models A–B.

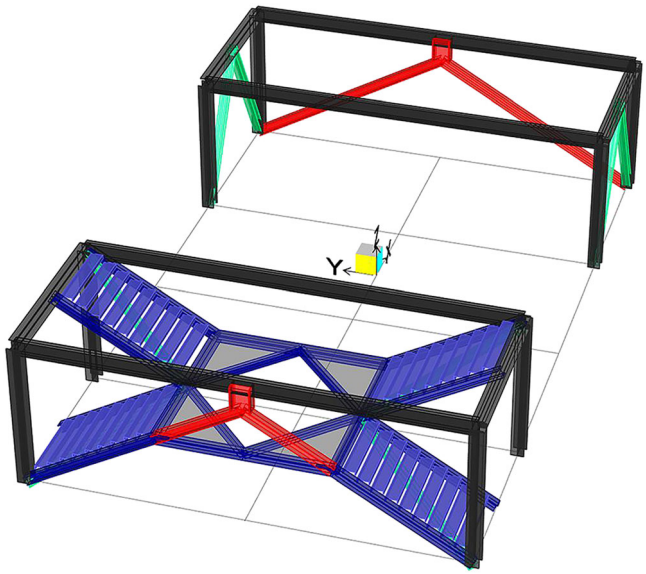

FIGURE 2 Typical braced frames (a) versus special braced stairs (b)

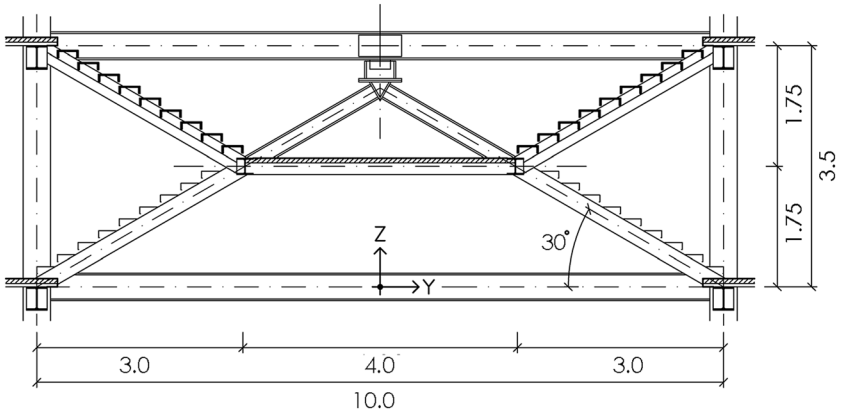

FIGURE 3 YZ elevation of the special braced stairs

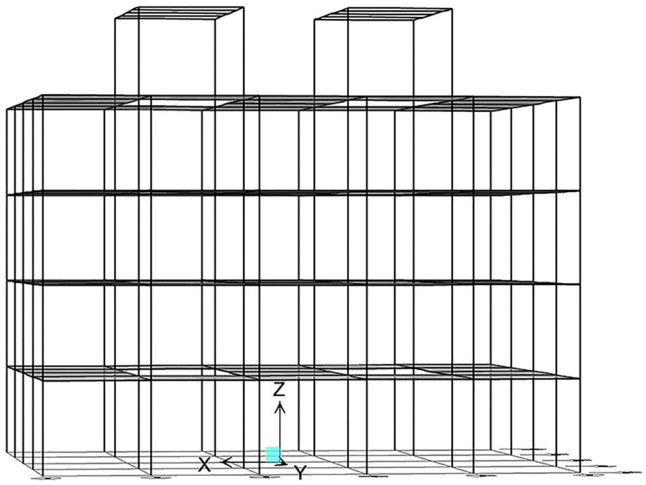

FIGURE 4 3D view of the main structure of the reduced analysis Models A–B

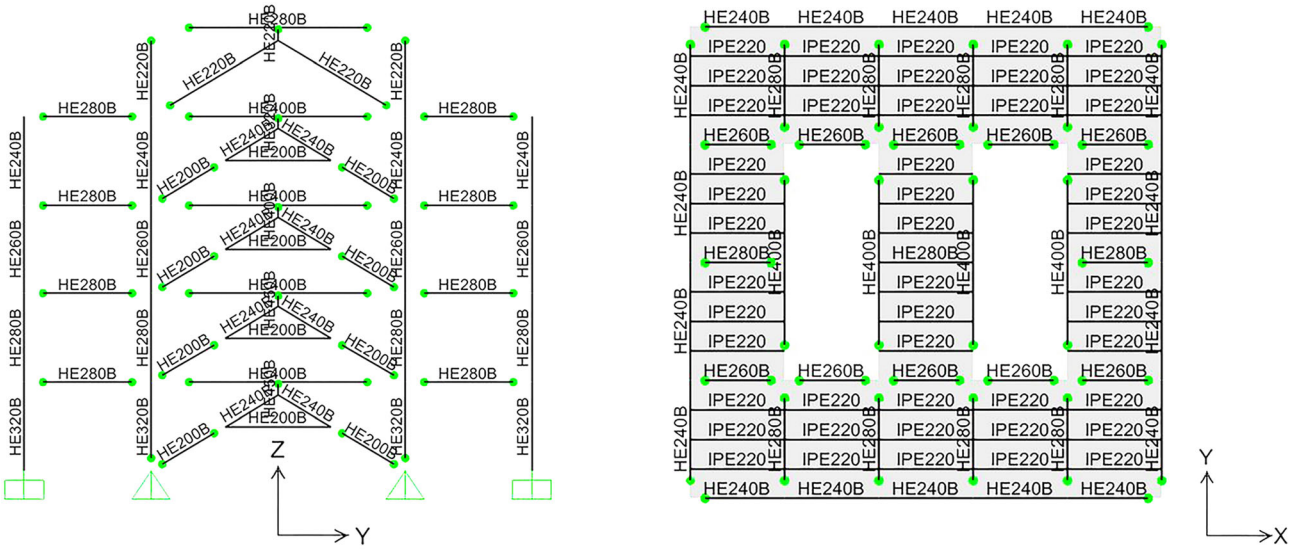

***(a)** Model B. YZ frame elevation* ***(b)** Typical (reduced) floor plant. Models A-B*

FIGURE 5 Cross-section sizes and joint releases

TABLE 1 Geometry of the main structure

Element	Units	X(*m*)	Y(*m*)	Z(*m*)
N. Storys	4			
Floor Dim		20	20	
Bays XZ	5	4		
Bays YZ	4		5	
Stairwells	2	4	10	
Height *h*	5			3.5

3.2.1 | Model A

Figure 6 shows the geometry of Model A (the reference structure). Stairs are considered nonstructural elements (not modeled in the seismic analysis). The bracing systems (IV-CBF and EBF) were designed according to specific rules for steel buildings (EC8). Characteristics of Model A:

- X-direction: Inverted-V concentrically braced frames (IV-CBF)/Slope $\alpha = 60°$/Length $l = 4$ m.
- Y-direction: Eccentrically braced frames (EBF)/Slope $\alpha = 30°$/Length $l = 5.8$ m/Vertical link $e = 50$ cm.
- All facades are moment-resisting frames (MRF).

3.2.2 | Model B

Figure 7 shows the geometry of Model B. Stairs are considered primary elements since they are part of the lateral force-resisting system. The same diagonals IV-CBF defined in Model A were relocated to the stairs (as shown in Figure 2). The length and cross-section size of concentric

TABLE 2 Cross-section size of steel elements

Column Level		Beam X	Girder Y		Beam Facades
			Sides	Central	
V	HEB 220	HEB 240		HEB 280	
IV	HEB 240	HEB 260	HEB 280	HEB 400	HEB 240
III	HEB 260	HEB 260	HEB 280	HEB 400	HEB 240
II	HEB 280	HEB 260	HEB 280	HEB 400	HEB 240
I	HEB 320	HEB 260	HEB 280	HEB 400	HEB 240

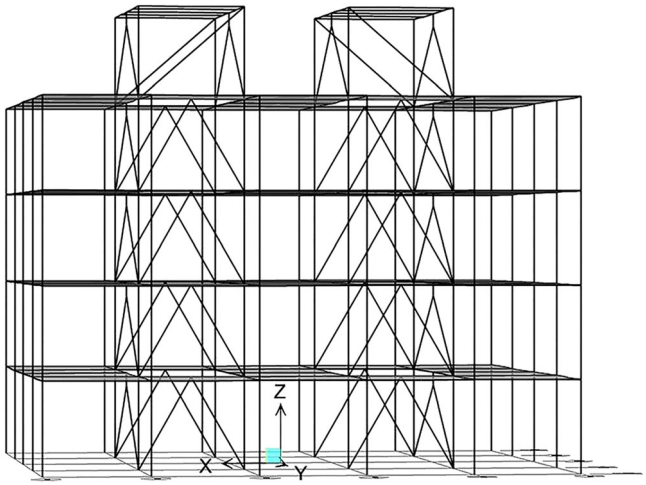

FIGURE 6 3D view of the reduced Model A

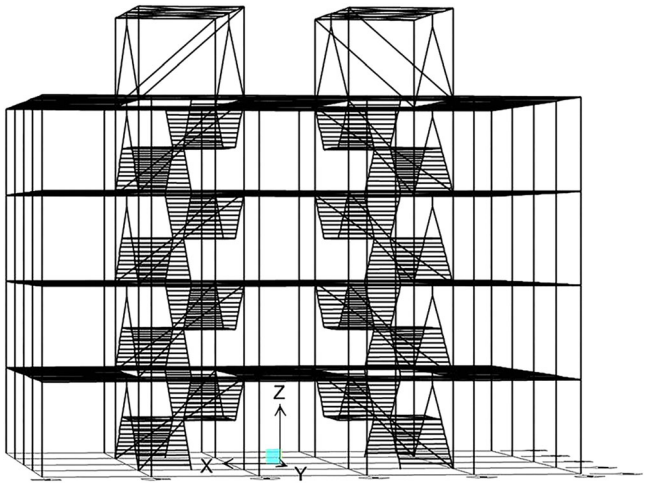

FIGURE 7 3D view of the reduced Model B

diagonals in the stair ramps are equal to Model A (IV-CBF). Note that part of the eccentric diagonals defined in Model A is reused as stair stringers. Characteristics of Model B:

- X-direction: Concentric diagonals in stair ramps (CBFs)/Diagonals length $l = 4$ m (identical to Model A).
- Y-direction: Stairs and EBFs/ Slope $\alpha = 30°$/Stringer $l = 3.5$ m/Eccentric beam $l = 2.3$ m/Link $e = 50$ cm.
- All facades are moment-resisting frames (MRF).

3.3 | Design rules for steel bracings (EC8)

Figures 8 and 9 show the flowcharts of the EC8-specific rules for the design of steel bracing systems proposed in the reference Model A (IV-CBF and EBF). However, the Model B stair system is not recognized by the seismic standard as a bracing system. Therefore, the comparative study has been based on integrating the same Model A bracings (designed according to EC8) into the stair structure of Model B.

3.3.1 | Design of concentric diagonals (CBF)

Figure 8 shows a flowchart of the EC8-specific rules for the design of inverted-V concentric bracings (with seismic energy dissipation in tension and compression diagonals) of the reference Model A. The design of these elements complies with three main conditions:

- The non-dimensional slenderness $\bar{\lambda}$ should be less than or equal to 2,0 *(6.7.3, EC8)*:

$$\bar{\lambda} \leq 2{,}0 \tag{4}$$

- Flexural buckling $N_{b,Rd}$ should be verified in compression diagonals according to *6.3.1, EC3*[26]:

$$N_{b,Rd} \geq N_{Ed} \tag{5}$$

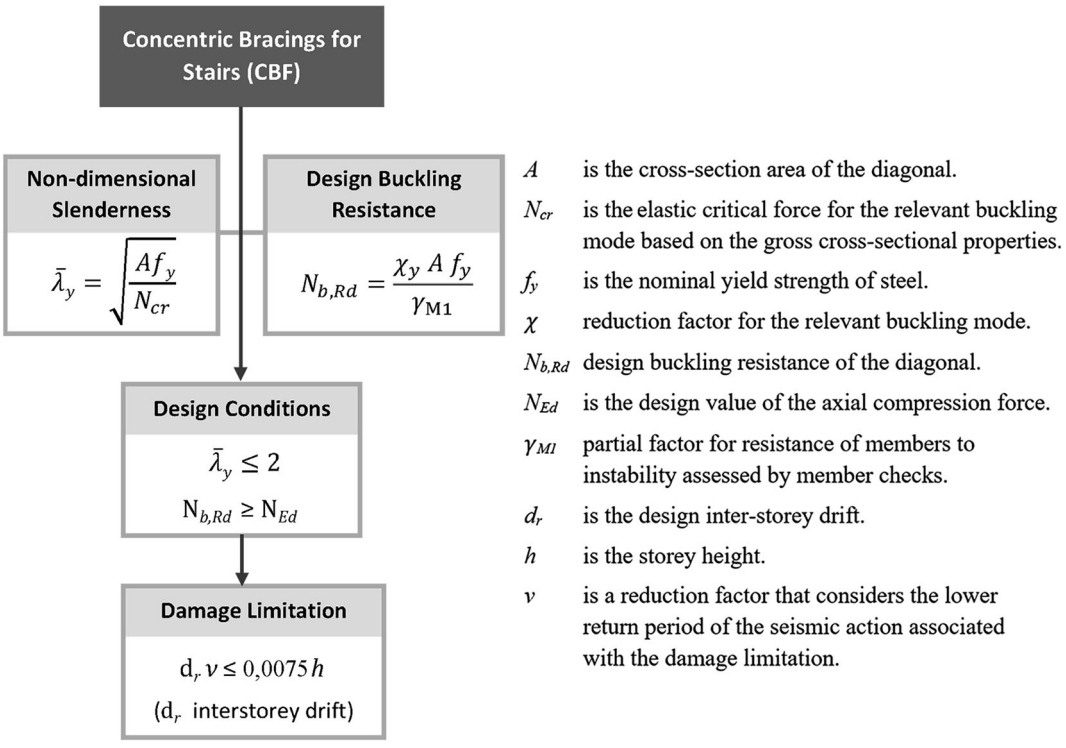

FIGURE 8 Design of inverted-V concentric diagonals (IV-CBF)

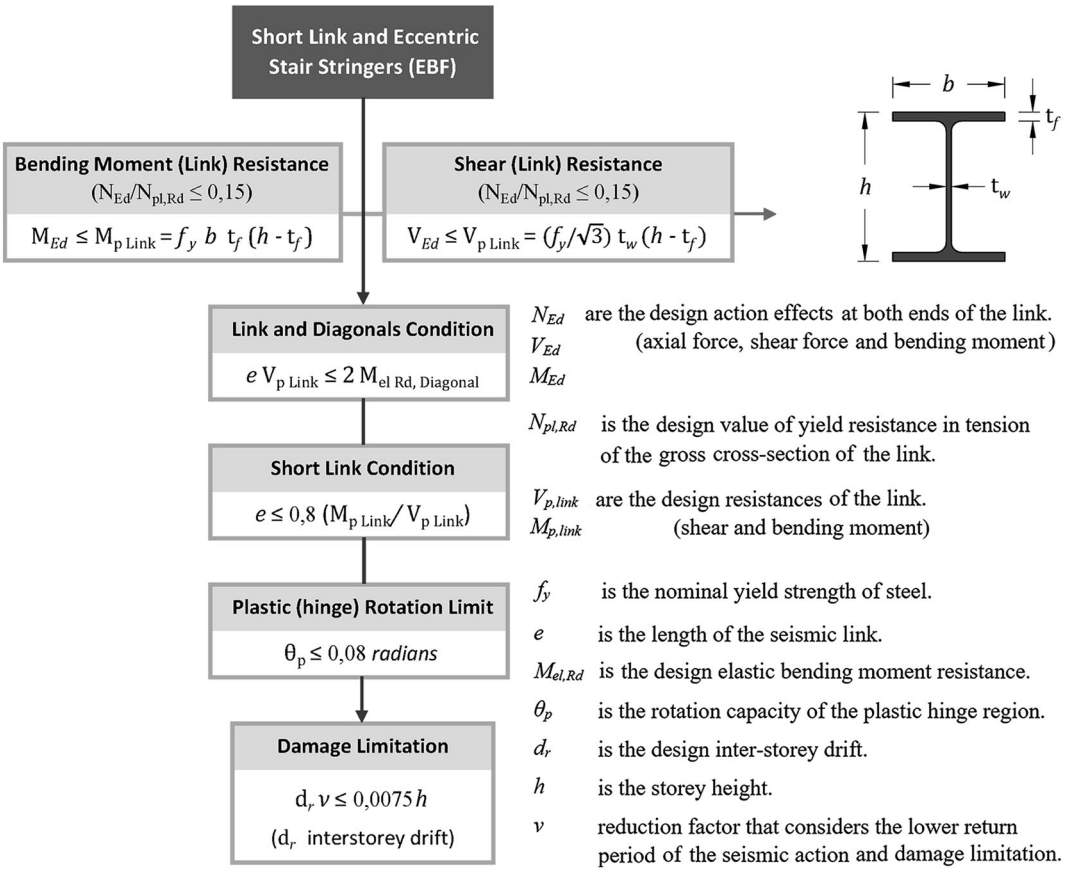

FIGURE 9 Design of eccentrically braced frames (EBF)

- The IV-CBFs should guarantee the *IDR* according to the *Damage limitation (4.4.3.b, EC8)*.

3.3.2 | Design of eccentric diagonals (EBF)

Figure 9 showed the flowchart for the design of vertical links hinged at their connection to the beam based on previous scientific and technical reports.[27] The design of the eccentric diagonals with a vertical link (Model A) complies with four main conditions:

- The shear plasticization of vertical links should avoid the elastic failure of diagonals:

$$e\,V_p \le 2\,M_{el,Rd} \tag{6}$$

- Vertical links are designed according to short links condition *(6.8.2*, [9], *EC8)*:

$$e \le 0{,}8\,(M_{pl}/V_{pl}) \tag{7}$$

- Plastic (hinge) nonlinear rotation θ_p in the rigid joint of seismic links should be limited to *(6.8.2* [10], *EC8)*:

$$\theta_p \le 0{,}08\,rad \tag{8}$$

- The EBFs should ensure the *IDR* according to the *Damage limitation (4.4.3.b, EC8)*.

3.4 | Steel bracings members. Models A–B

Figure 10 shows the braced frames of Models A–B. Both systems are braced in the X-direction, by concentric diagonals (green), and in the Y-direction, by eccentric diagonals (red). Model B has the same steel bracing members of Model A integrated into the stair structure. Table 3 shows the steel cross-section size in bracings.

All members of the main structure (columns and beams), stairs stringers, and bracings were defined with HEB and S355 steel (only the stair rungs were modeled with UPE). The concentric diagonals of both models were defined with different section sizes on each floor. All eccentric diagonals were HEB 240 section size. The vertical links have different cross-section size at each level. All steel bracings were modeled with pinned end connections. At each story, the only rigid connections were the union between the vertical link and the eccentric diagonals as well as the moment-resisting frames (MRF) in façades. Table 4 shows the steel weight of the concentric diagonals. Both Models A–B has identical concentric diagonals. Hence, the comparative study of the eccentric diagonals is decisive. Table 5 shows the steel weight of the eccentric diagonals. The steel members of Model B used as stairs stringers (Y-direction) are not computed as bracing members. Therefore, Model B takes advantage of the stair structure to reduce the amount of steel in the eccentrically braced frame system (EBFs).

3.5 | Plastic hinges. Models A–B

3.5.1 | Plastic hinges in stairs and main structure

In order to compare both models, the seismic behavior factor *R* has been analyzed. To do so, it has been modelled the nonlinear response by preventing failures in the stairs and main structure. The plastic hinges in steel elements were defined with the structural analysis program Sap2000, according to the modeling parameters and acceptance criteria of the FEMA 356 document. Pre-qualified joints were modeled according

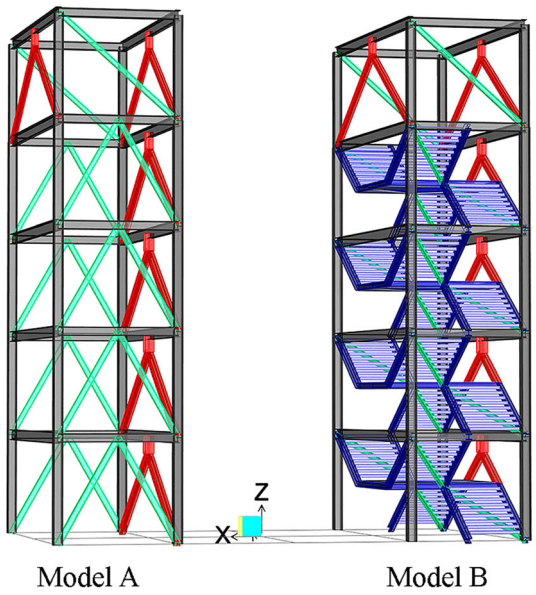

FIGURE 10 3D view of both steel bracing systems

TABLE 3 Cross-section size of steel bracings

Level	Stairs Stringer	Concentric bracing	Eccentric bracing	
			Link	Diagonal
V		HEB 140	HEB 240	HEB 240
IV	HEB 200	HEB 120	HEB 320	HEB 240
III	HEB 200	HEB 140	HEB 400	HEB 240
II	HEB 200	HEB 160	HEB 400	HEB 240
I	HEB 200	HEB 180	HEB 450	HEB 240

TABLE 4 Weight of concentric diagonals

Section size	HEB 200–120
Weight/m (medium)	38.5 kg/m
Length	3.95 m
Weight/bracing	152 kg
Units (Levels I–IV)	32
Total Weight	4.864 kg
Steel reduction ratio	-

TABLE 5 Weight of eccentric diagonals

Section size	HEB 240	
Weight/m	83.2 kg/m	
Model	**A**	**B**
Length	5.83 m	2.43 m
Weight/bracing	485 kg	202 kg
Units (Levels I–IV)	16	16
Total weight	7.760 kg	3.232 kg
Steel reduction ratio	58.4%	

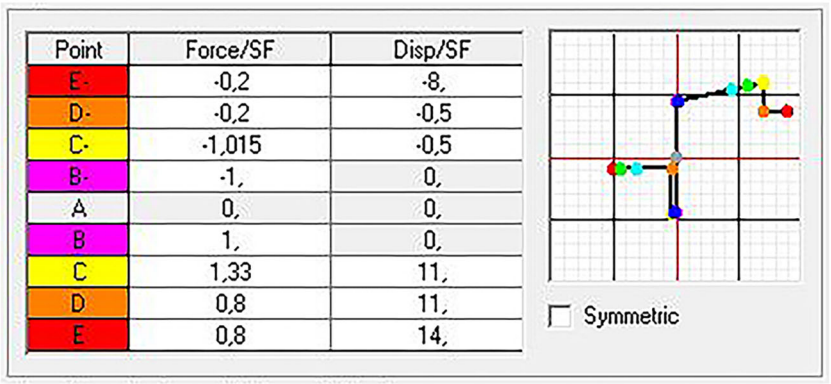

FIGURE 11 Plastic hinge force–displacement diagram. IV-CBF

to FEMA 350.[28] The expected result of the pushover analysis is to concentrate all the seismic performance on the seismic dissipative members. Thus, except for these elements (explained below), all plastic hinges were defined at the ends of steel members of the main structure (columns and beams), stairs (stringers and rungs), and eccentric diagonals, according to the degrees of freedom (DOF) related to P-M2-M3 (interaction of axial forces and bending moments).

3.5.2 | Plastic hinge in concentric diagonals (IV-CBF)

Figure 11 shows the asymmetric response of the plastic hinge diagram (Force–Displacement), depending on whether diagonals are subjected to tension or compression axial force *(Table 5.6, FEMA 356)*. The plastic hinge of the concentric bracing (with seismic energy dissipation in tension and compression) was defined at the center of the diagonal, according to the DOF related to P (axial).

3.5.3 | Plastic hinge in seismic links (EBF)

Figure 12 shows the parameters of the plastic hinge in seismic energy dissipators designed as short links *(6.8, EC8)*. The vertical links behave as seismic fuses (easy to repair) that prevent damage and deformation of the stairs and main structure. The pure bending moment in short links generates

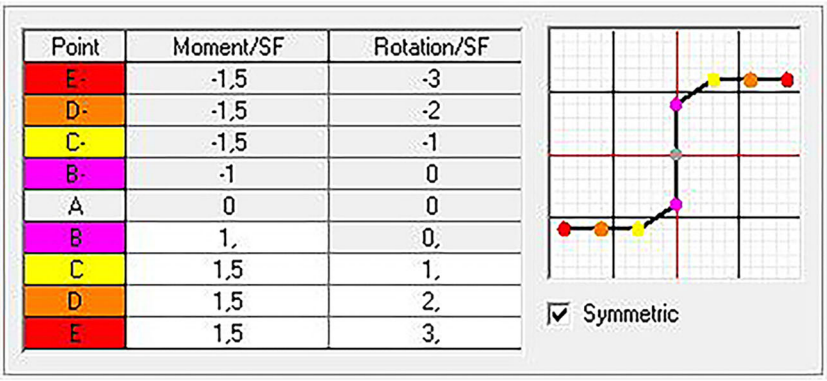

FIGURE 12 Plastic hinge force–displacement diagram. Link EBF

TABLE 6 Building and ground properties

Permanent loads G	
Floors and stairs (finishes and partitions)	2 kN/m^2
Façades (light panels)	2 kN/m
Live loads Q	
Floors and stairs	3 kN/m^2
Ground characteristics (EC8)	
Basic acceleration (PGA-475)	0.42*g*
Class of design spectrum	Type 1
Ground type	*C*
Building characteristics	
Total weight	11.810 kN
Importance factor (building class III)	$\gamma_1 = 1.0$
Viscous damping ratio	$\xi = 0.05$

plasticity by shear force. Hence, the DOF related to M3 allows nonlinear behaviour. The limitation of plastic rotation for short links is $\theta_p \leq 0{,}08$ *rad* (EC8); the overstrength value is 1,5. The controlling plastic mechanism of the dual system (stairs stringers and eccentrically braced frames) was checked in the pushover analysis to ensure the invariant kinematic response of the structure.[29,30] Recent articles studied the effects of the strength of steel in vertical links on the seismic behavior of the building.[31–33] Satisfactory results were obtained considering S355 steel for the seismic links.

3.6 | Building, ground, and material properties

Table 6 summarizes the main analysis data. The self-weight of the structural elements was automatically calculated by the structural analysis program. The permanent loads G are typical values of light-construction systems. The live loads Q on floors and stairs correspond to school use. The floor and building characteristics are defined below (Table 6). Table 7 shows the material properties of the steel S355 according to EC3.

4 | METHODOLOGY OF ANALYSIS

4.1 | Linear-elastic modal analysis

Linear-elastic modal analysis (4.3.3, EC8) was applied using the SAP2000 computer code[34] to check the deformed shape of stairs subject to the interaction of inertial forces and *IDR*. The definition of the stairs structure in the analysis model allows more realistic results.[35] The highest modes should be checked on models with stairs.[36] Initially, the interaction between the stairs and the main structure was checked considering the first 12 modes of vibration (four story $\times$ 3DOF(U_x,U_y,R_z) = 12 modes). The lateral drifts of stairs landings and the influence of the staircases on the

TABLE 7 Material properties

Material	Steel
Type	S355
Reference	EN 10025-2
Weight per unit volume (kN/m^3)	76.97
Mass per unit volume (kg/m^3)	7.849
Modulus of elasticity, E (N/mm^2)	210.000
Poisson's ratio, U	0.30
Shear modulus, G (N/mm^2)	81.000
Minimum yield sress, F_y (N/mm^2)	355
Minimum tensile stress, F_u (N/mm^2)	510
Effective yield stress, F_{ye} (N/mm^2)	390.5
Effective tensile stress, F_{ue} (N/mm^2)	561

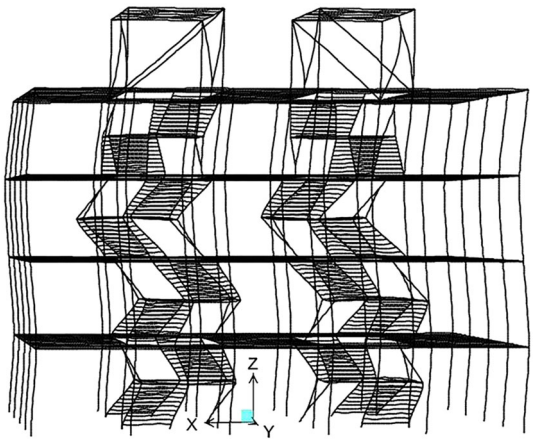

FIGURE 13 Seventh vibration mode of an initial prototype

vibration periods of the building were analyzed. The eigenvalue modal analysis was mainly performed to determine the modes, their corresponding modal participation factors, and the natural periods of vibration. As an example, Figure 13 shows a prototype considering the seventh vibration mode of the building. Note that the response of each stair landing is decoupled from the drift of its respective floor. That is, the lateral displacements of the stair landings (larger than the *IDR*) allow checking the lack of lateral stiffness in stairs. This undesirable response was prevented by integrating the concentric diagonals of reference Model A into the stair structure of Model B.

4.2 | Static nonlinear (pushover) analysis

As commented above, the results of the nonlinear analysis (plastic mechanisms, damage distribution, and seismic behavior) in models with stairs are more realistic and accurate. The spatial (3D) models subjected to constant (vertical) gravity loads, and incremental (horizontal) ones in each principal direction (X–Y), were analyzed. The lateral loading pattern allows representing increasing seismic forces. The displacement of the roof with respect to the base shear force defines the capacity curve: the initial linear-elastic response and the subsequent nonlinear response. In Model A, the unfavorable interaction between stairs and the main structure could not be checked (damage to stairs is uncertain). Model B (with stairs) avoids uncertainties:

a. Effects caused by the stairs on the main structure:

- Lateral stiffness changes in frames
- Regularity and symmetry changes

- Accidental torsional effects
- Short columns and eccentric beams

b. Effects caused by the main structure on the stairs:

- Stair landing acceleration
- Stair stringer deformation

4.3 | Estimation of the performance point

In order to estimate the maximum roof displacement, the graphical procedure of the *Capacity spectrum method (ATC-40)* has been employed. As stated in document FEMA 440,[37] the *Capacity spectrum method* assumes that the equivalent damping of the system is proportional to the area enclosed by the capacity curve. The equivalent period T_{eq} is assumed to be the secant period T_{sec} at which the seismic ground motion demand (reduced by the equivalent damping β_{eq}) intersects the capacity curve. Since both the equivalent period and the damping depend on the displacement, the solution to determine the maximum inelastic displacement (i.e., performance point) is iterative. Using the structural analysis program Sap2000, the maximum spectral displacement was determined according to the ATC-40 equivalent linearization procedure using the values of the principal parameters $T_{eq} = T_{sec}$ and β_{eq}. The damage limitation according to *IDR* and the *LS* performance level in structural and nonstructural elements should be verified.[38] That is, the performance point should not exceed the damage limitation (EC8) or *CP* performance level (FEMA 356).

4.4 | Analysis of behavior factor R

The inelastic control of steel buildings is based on the capacity (ductility and overstrength) of certain predefined structural types (*Chapter 6, EC8*). For these reference types, the design seismic forces can be obtained by reducing the elastic spectrum by the behavior factor *R*, which accounts for ductility and the dissipative capacity of the structural system. The calculation of the behavior factor *R* as a function of the maximum roof displacement can be determined graphically. Figure 14 shows the graphical procedure for calculating the factor *R*. The equivalent linear-elastic force V_E is obtained from the elastic stiffness K_{el} and maximum roof displacement Δ_{max}.

$$V_E = K_{el}\ \Delta_{max} = (V_d/\Delta_d)\,\Delta_{max} \tag{9}$$

where V_d is the design lateral force, Δ_d is the design displacement, and Δ_{max} is the maximum displacement at the roof. Knowing the value of the equivalent linear-elastic force V_E regarding the maximum displacement Δ_{max}, and the base shear V_d corresponding to the design forces (in this case, the limit point of the elastic response), the seismic behavior factor *R* is determined as follows:

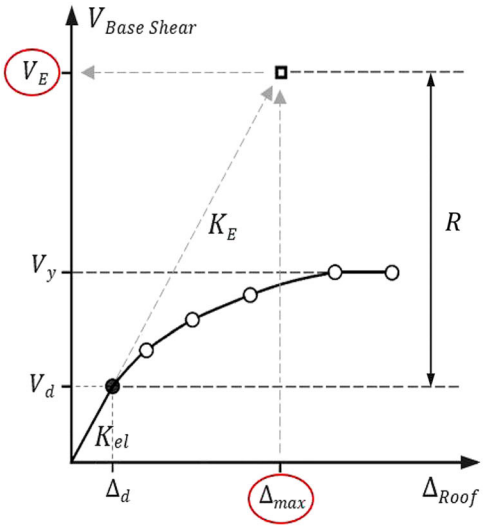

K_{el}	*Elastic response of structure*
K_E	*Equivalent-elastic response*
V_d	*Design force/yield strength*
V_y	*Fully yielded strength*
V_E	*Equivalent-elastic force (seismic demand)*
Δ_d	*Drift under design force*
Δ_{max}	*Maximum drift (seismic demand)*
R	*Behavior factor*

FIGURE 14 Behavior factor R (FEMA P-750)

$$R = \frac{V_E}{V_d} \tag{10}$$

The upper limit of reference values of behavior factors R (for systems regular in elevation) is defined according to the structural type. These values are assigned concerning the ductility class medium (DCM) or high (DCH). The reference values of R for typical braced frames are predefined in *Table 6.2*, *EC8*. Thus, in the X-direction, the behavior factors values for the IV-CBFs are R_{DCM} =2 and R_{DCH} =2,5. In the Y-direction, the behavior factor values for the EBFs are R_{DCM} =4 and R_{DCH} =5(V_y/V_d), where the ratio (V_y/V_d) is the plastic redistribution parameter defined as overstrength. However, EC8 does not provide the reference behavior factor R for the braced stair system. Therefore, nonlinear static (pushover) analysis is used to estimate the ductility and dissipation capacity of the bracing members in stairs (Section 5).

4.5 | Dynamic analysis of stairs

Dynamic analysis has been performed with the SAP2000 program and the same 3D analytical models used in the pushover analysis. The time history analysis *(4.3.3.4.3, EC8)* is a step-by-step procedure to consider the dynamic response of a structure to a specific load (ground motion) varying as a function of time. The considered ground motion (PGA = 0.36*g*) corresponds to the North-South component of El Centro (1940) earthquake. The nonlinear time-history analysis (NLTHA) used the *Direct integration method*. Eigenvectors were selected to determine the shapes of the undamped free vibration modes of the system. This methodology is effective for models whose structural response is mainly linear elastic, except for specific elements acting as seismic energy dissipators (CBFs and EBFs). NLTHA allows considering the material (S355 steel) and geometric (P-delta) nonlinearity. Analytical tools incorporating material and geometric nonlinearities can estimate the main features related to the seismic behavior of the diagonals in CBF.[39] The NLTHA focused on the dynamic response of stairs components higher sensitive to deformation (concentric diagonals and vertical links) and acceleration (stair landings). Figure 15 shows El Centro accelerogram used as the reference earthquake.

4.6 | Pilot study considerations

4.6.1 | Analysis models

Torsional characteristics of reduced analysis models

The arrangement of the vertical bracing cores located close to the periphery of the building has clear advantages (in accordance with *4.2.1.4*, *Torsional resistance and stiffness*, *EC8)*. Therefore, it is assumed that the archetype (Figure 1a) should have adequate torsional stiffness to limit the development of torsional movements. However, the vertical bracing cores of the reduced analysis model (Figure 1b) are centralized in the plan and have less torsional inertia concerning the archetype. Since the analysis is focused on the direct relationship between the relative drifts between floors (in the principal X–Y-directions) and the local capacity of the primary elements in the bracing systems, the specific global-torsional characteristics of the reduced models are not relevant to the research and should be neglected.

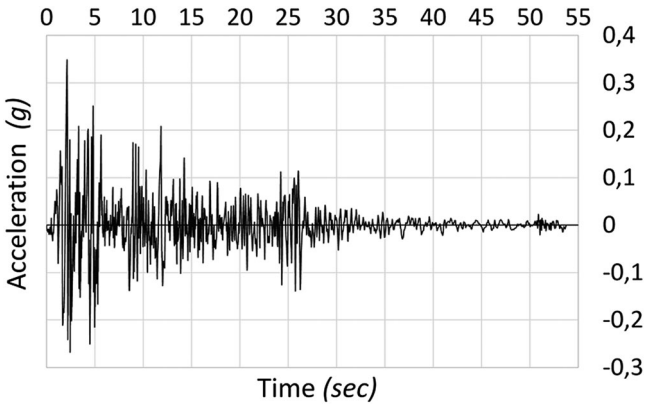

FIGURE 15 El Centro earthquake (1940). North-South component

Assumptions on stairs of Model A

The structure of buildings is usually analyzed using idealized models without stairs (as stated in the previous Section 2 Seismic standard review). Model A without stairs corresponds to this classical approach. According to the seismic standard, it is assumed that the stairs of Model A do not influence the lateral force-resisting system (ATC-40) and are isolated from the main structure (FEMA 356). If the *Damage limitation (4.4.3.2, EC8)* is respected, it may be assumed that stairs should tolerate the (design) inter-story drifts. Model A stairs should have adequate anchorage and bracings (FEMA 750) and sliding connections that should tolerate displacements larger than the design *IDR* (FEMA E-74). It is assumed that the unmodeled-isolated stairs of Model A do not suffer local damage nor cause alterations in global behavior. However, Model B should verify the effectiveness of the braced stair system subjected to *IDR* in two main X–Y-directions.

4.6.2 | Methods of analysis

Estimation of torsional effects (Pushover analysis)

Section *4.3.3.4.2.2 Lateral loads (EC8)* states that the modal pattern used in the pushover analysis can be defined according to *4.3.3.2 Method of lateral force analysis (EC8)*. Since the shape of the fundamental mode is approximated by the horizontal displacements of the diaphragms (which increase linearly along the height), the criterion for defining the lateral loads correspond to *4.3.3.2.3* [3] *Distribution of the horizontal seismic forces (EC8)*. The modal analysis allows checking several conditions for the application of the pushover method. Initially, the sum of the effective modal masses for the modes considered should amount to at least 90% of the total mass *(4.3.3.3.1* [3] *General, EC8)*. If this is not fulfilled due to the contribution of torsional modes, the minimum number of modes considered k in the 3D analysis should satisfy *(4.3.3.3.1* [5], *EC8)*:

$$k \geq 3\sqrt{n} \text{ where } n \text{ is the number of storeys, and the period of the } k \text{ mode satisfy } T_k \leq 0{,}2\,s \tag{11}$$

The response of two vibration modes i and j (including both translational and torsional modes) may be considered independent if their periods satisfy the following condition *(4.3.3.3.2* [1], *EC8)*:

$$T_j \leq 0{,}9\,T_i \qquad \text{where } T_j \leq T_i \tag{12}$$

As established, regular models are not significantly affected by the contributions of the modes superior to the fundamental mode in each main direction (X–Y) if their fundamental periods of vibration T_1 satisfy the condition *(4.3.3.2.1* [2], *EC8)*:

$$T_1 \leq [4 \cdot T_C; 2,0\ sec] \text{ where } T_C = 0{,}6\ sec \quad \text{according to } Table\ 3.2\ (EC8). \tag{13}$$

Initially, when pushover analysis is performed with the force patterns specified in *4.3.3.4.2.2* (EC8) may significantly underestimate deformations at the stiff/strong side in one direction of the structure (with a predominately torsional second mode of vibration). For such structures, displacements at the stiff/strong side shall be increased, compared to those in the corresponding torsional balanced structure *(4.3.3.4.2.7 Procedure for the estimation of the torsional effects, EC8)*. This requirement is deemed to be satisfied if the amplification factor to be applied to the displacements of the stiff/strong side is based on an elastic modal (3D) analysis. However, the specific global-torsional characteristics of the reduced Models A–B are not representative of archetype behavior and should be neglected. Since Models A–B satisfy the previous conditions (Eqs. 11,12, and 13), the pushover method was applied considering the first translational mode in each main direction (U_x,U_y). Note that the pushover method has been only used to predefine the cross-section size of the steel elements and other basic properties (weight of diagonals, elastic stiffness, and behavior factor R). Thus, the main results (maximum *IDR*, forces in bracings, and plastic rotations in hinges) were obtained by the NLTHA.

Vertical component of the seismic action (Dynamic analysis)

Section *4.3.3.5.2 Vertical component of the seismic action (EC8)* states that if the design ground acceleration in the vertical direction a_{vg} is greater than 0.25g, it should be considered in some specific cases. Although stairs are not mentioned, the effects of the vertical component should not be overlooked. However, in accordance with *4.3.3.5.2* [5], if pushover analysis is performed, the vertical component may be neglected.

5 | COMPARATIVE ANALYSIS. MODELS A–B

5.1 | Linear-elastic modal analysis

Table 8 shows that Model A has higher lateral stiffness on the X-axis than Y-axis. However, the stiffness of Model B on the X-axis is lower than Y-axis. The fundamental period is generated in axes with lower stiffness: Y-axis in Model A (T_1=0.696 s) and X-axis in Model B (T_1=0.734 s). The second vibration mode generates a global torsion around the Z-axis (it may be neglected). The third mode corresponds to the stiffest axis (U_x in Model A and U_y in Model B). Table 9 shows the modal participating mass ratios. As expected, the participating mass ratio in the fundamental mode of four-story braced buildings (such as Models A–B) does not reach 90% of the total mass. However, in low-rise buildings, the modal response is usually very basic, and translational Modes 1 and 3 can be considered representative of the main response, according to

- In four-story (3D) models, considering $k = 6$ first modes, 90% of the total mass is reached *(4.3.3.3.1, EC8)*.
- Archetype buildings are not affected by the specific torsional modes of reduced models *(4.2.1.4, EC8)*.
- All modes can be considered independent of each other *(4.3.3.3.2* [1], *EC8)*.
- First translational modes are not significantly affected by contributions of higher modes *(4.3.3.2.1, EC8)*.

5.2 | Pushover analysis

5.2.1 | Model A/Push X

Figure 16a illustrates the graphical procedure of the *Capacity-spectrum method* (ATC-40). The initial capacity (pushover) curve and EC8 demand spectrum (Table 6) were converted into *ADRS* format and superimposed on the diagram defined in *Spectral displacement (m)/Spectral acceleration (g)* coordinates. The spectral yield point (0.028 m; 0.653*g*) and spectral displacement point (0.068 m; 0.716*g*) defined the bilinear representation

TABLE 8 Linear-elastic modal analysis

Model Elastic stiffness K_{el} (kN/m)	A	B
X-axis	144.086	64.109
Y-axis	77.697	133.600
Periods of vibration T_i (s)		
Mode 1	$U_y = 0.696$	$U_x = 0.734$
Mode 2	$R_z = 0.577$	$R_z = 0.617$
Mode 3	$U_x = 0.476$	$U_y = 0.516$
Mode 4	$U_y = 0.347$	$U_x = 0.354$
Mode 5	$R_z = 0.242$	$R_z = 0.251$
Mode 6	$U_x = 0.139$	$U_y = 0.150$

TABLE 9 Modal participating mass ratios

Model Sum U_x	A	B
	Mode 3 = 0.79	Mode 1 = 0.81
	Mode 6 = 0.90	Mode 4 = 0.92
Sum U_y		
	Mode 1 = 0.89	Mode 3 = 0.86
	Mode 4 = 0.97	Mode 6 = 0.95

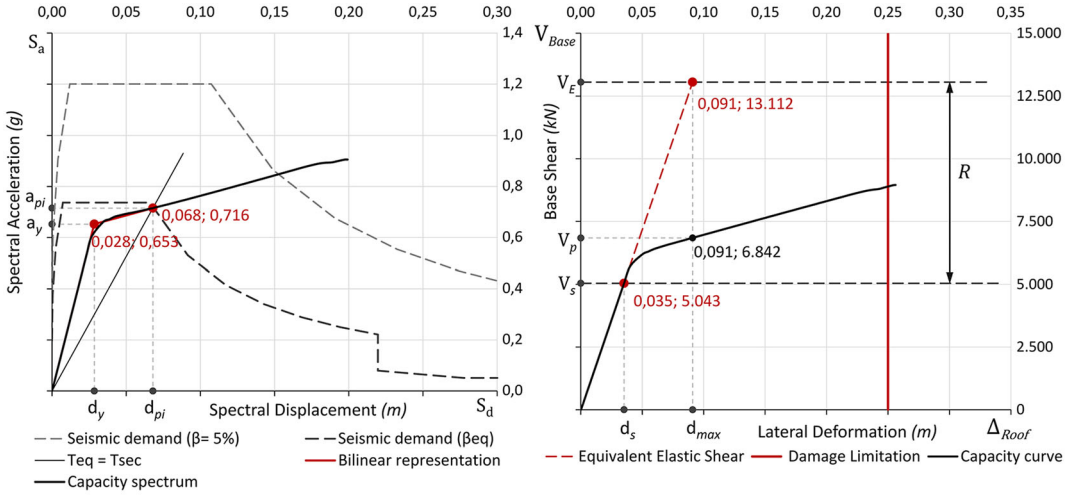

(a) Spectral displacement *(b) Capacity (Pushover) curve*

FIGURE 16 Model A/Push X

TABLE 10 Seismic analysis of Model A/Push X

Capacity spectrum. Bilinear representation		
	S. Displacement (m)	**S. Acceleration (*g*)**
Yielding point	0.028	0.653
Performance point	0.068	0.716
Maximum spectral displacement		
Effective period (s)	T_{eq}	0.615
Effective damping	β_{eq}	0.245
Behavior factor R. Computation parameters		
	Displacement (m)	Base shear (kN)
Elastic limit point	0.035	5.043
Equivalent linear point	0.091	13.112
Structural behavior characteristics		
Elastic stiffness K_{el} (kN/m)		144.086
Behavior factor R		2.60

of the capacity spectrum, to obtain the effective period ($T_{eq} = 0.615$ s) and damping factor ($\beta_{eq} = 0.245$). These two parameters (T_{eq}, β_{eq}) determine the maximum spectral displacement.

Figure 16b shows the performance point (0.091 m; 6.842 kN) on the capacity curve, regarding the damage limitation *(4.4.3.2.b, EC8)*. The linear-elastic stiffness $K_{el} = V_s/d_s$ was calculated $K_{el} = 144.086$ kN/m. Then, the equivalent linear-elastic force at the performance point $V_E = K_{el}$ d_{max} was computed $V_E = 13.112$ kN. The behavior factor was obtained by dividing V_E by the base shear at the elastic limit point $V_s = 5.043$ kN.

Table 10 shows the highest elastic stiffness K_{el} and the lowest behavior factor of the research: $R = 2.60$.

5.2.2 | Model A/Push Y

Figure 17a shows the initial capacity curve and demand spectrum in *ADRS* format. The spectral yield point (0.030 m; 0.283*g*) and spectral displacement point (0.120 m; 0.620*g*) defined the bilinear representation of the capacity spectrum, for the calculation of the effective period ($T_{eq} = 0.884$ s) and the damping factor ($\beta_{eq} = 0.136$). These parameters confirmed the maximum spectral displacement (0.120 m; 0.620*g*) according to the spectral demand.

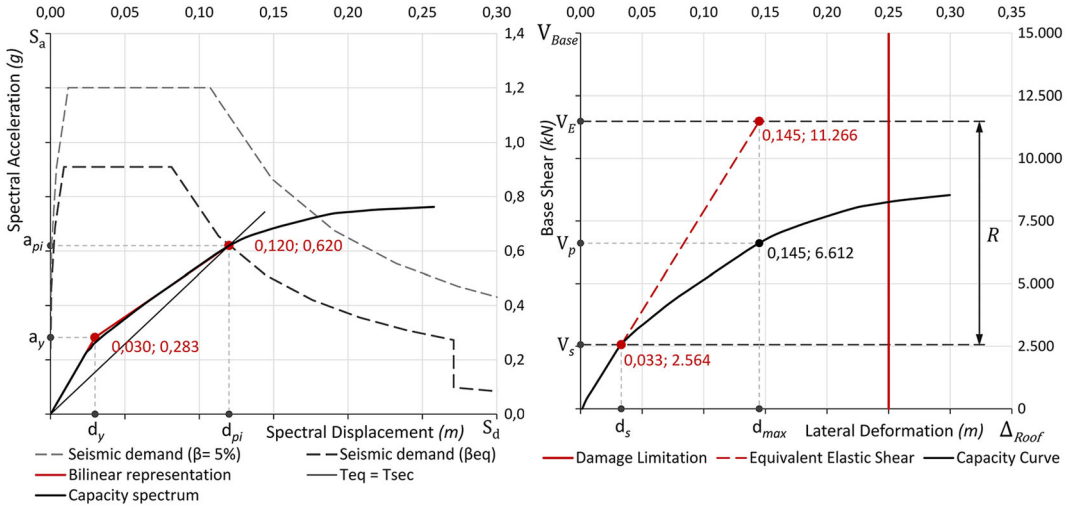

(a) Spectral displacement *(b) Capacity (Pushover) curve*

FIGURE 17 Model A/Push Y

TABLE 11 Seismic analysis of Model A/Push Y

Capacity spectrum. Bilinear representation		
	S. displacement (m)	**S. acceleration (*g*)**
Yielding point	0.030	0.283
Performance point	0.120	0.620
Maximum spectral displacement definition		
Effective period (s)	T_{eq}	0.884
Effective damping	β_{eq}	0.136
Behavior factor R. Computation parameters		
	Displacement (m)	Base shear (kN)
Elastic limit point	0.033	2.564
Equivalent linear point	0.145	11.266
Structural behavior characteristics		
Elastic stiffness K_{el} (kN/m)		77.697
Behavior factor R		4.39

Figure 17b shows the capacity (pushover) curve and the localization of the performance point (0.145 m; 6.612 kN), according to the damage limitation. The linear-elastic stiffness value is $K_{el} = 77.697$ kN/m. The equivalent linear-elastic force at the performance point was calculated $V_E = 11.266$ *kN*. Dividing V_E by the base shear at the yielding point Vs = 2.564 kN, the behavior factor *R* was obtained. Table 11 summarizes each parameter to obtain the behavior factor at the performance point $R = 4.39$.

5.3 | Pushover analysis. Model B

5.3.1 | Model B/Push X

Figure 18a shows the capacity curve and demand spectrum in *ADRS* format. The spectral yield point (0.05 m; 0.536*g*) and spectral displacement point (0.106 m; 0.931*g*) defined the bilinear representation of the capacity spectrum. The effective period ($T_{eq} = 0.676$ s) and the damping factor ($\beta_{eq} = 0.091$) confirmed the maximum spectral displacement, according to the seismic demand.

Figure 18b shows the performance point (0.128 m; 6.798 kN) concerning to damage limitation (4.4.3.2.2.b, EC8). The value of the linear-elastic stiffness is $K_{el} = 64.109$ kN/m. The equivalent linear-elastic force at this point was calculated $V_E = 8.206$ kN. The base shear value at the elastic limit point is $V_s = 2.949$ kN.

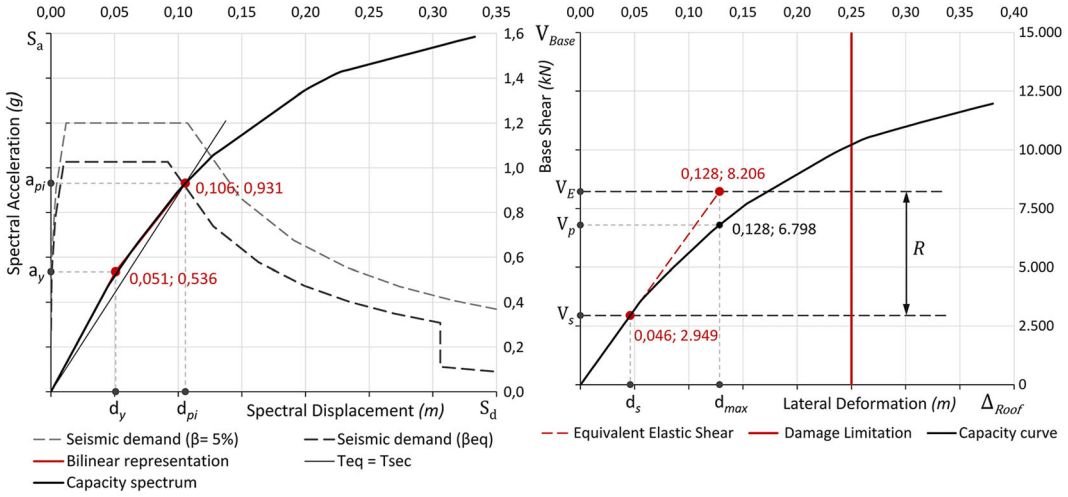

(a) Spectral displacement *(b) Capacity (Pushover) curve*

FIGURE 18 Model B/Push X

TABLE 12 Seismic analysis of Model B/Push X

Capacity spectrum. Bilinear representation		
	S. displacement (m)	**S. acceleration (*g*)**
Yielding point	0.051	0.536
Performance point	0.106	0.931
Maximum spectral displacement definition		
Effective period (s)	T_{eq}	0.676
Effective damping	β_{eq}	0.091
Behavior factor R. Computation parameters		
	Displacement (m)	Base shear (kN)
Elastic limit point	0.046	2.949
Equivalent linear point	0.128	8.206
Structural behavior characteristics		
Elastic stiffness K_{el} (kN/m)		64.109
Behavior factor R		2.78

Table 12 Although the bracings located in the stair ramps are identical to the inverted-V diagonals of Model A (the same cross-section size and length), this response verifies the minimum elastic stiffness $K_{el} = 64.109$ kN/m and the largest capacity curve of the comparative study (the roof displacement $d_{max} = 0.383$ m). The behavior factor at the performance point (according to seismic demand) is $R = 2.78$.

5.3.2 | Model B/Push Y

Figure 19a shows that Model B/Push Y analysis provides the most important results of the research. The spectral yield point (0.019 m; 0.357*g*) and spectral maximum displacement (0.091 m; 0.739*g*) defined the bilinear representation of the capacity spectrum. The effective period ($T_{eq} = 0.702$ *s*) and the damping factor ($\beta_{eq} = 0.167$) determine the maximum spectral displacement, according to seismic demand.

Figure 19b shows the performance point at the capacity curve (0.095 m; 6.081 kN) concerning damage limitation *(4.4.3.2.2.b, EC8)*. The value of the linear-elastic stiffness is $K_{el} = 133.600$ kN/m. The equivalent linear-elastic force at the performance point was calculated $V_E = 12.692$ kN. The behavior factor *R* was obtained by dividing V_E by $V_s = 2.004$ kN.

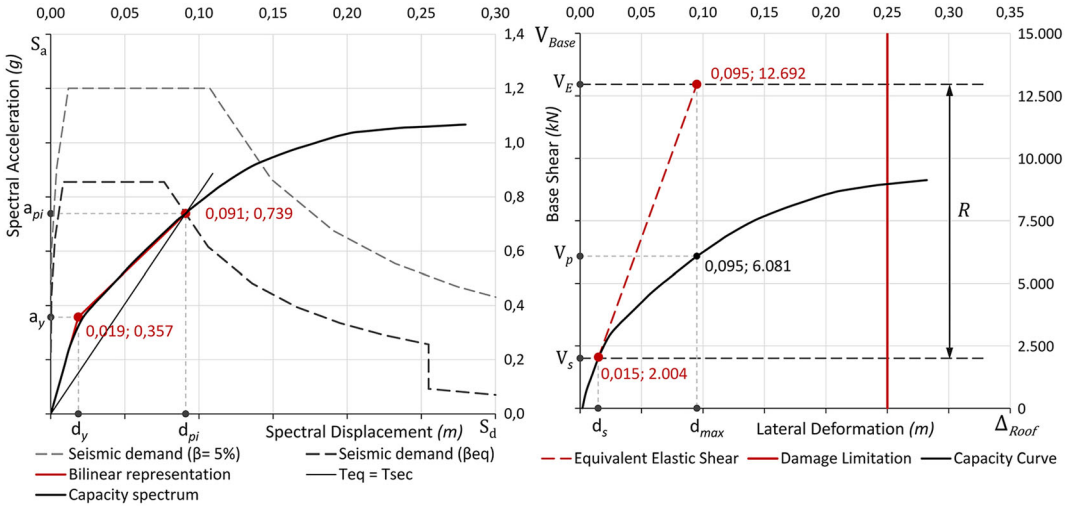

(a) Spectral displacement *(b) Capacity (Pushover) curve*

FIGURE 19 Model B/Push Y

TABLE 13 Seismic analysis of Model B/Push Y

Capacity spectrum. Bilinear representation		
	S. displacement (m)	**S. acceleration (*g*)**
Yielding point	0.019	0.357
Performance point	0.091	0.739
Maximum spectral displacement definition		
Effective period (s)		
Maximum spectral displacement definition		
Effective period (s)	T_{eq}	0.702
Effective damping	β_{eq}	0.167
Behavior factor R. Computation parameters		
	Displacement (m)	Base shear (kN)
Elastic limit point	0.015	2.004
Equivalent linear point	0.095	12.692
Structural behavior characteristics		
Elastic stiffness K_{el} (kN/m)		133.600
Behavior factor R		6.33

Table 13 summarizes all parameters. The Y-direction response of Model B, controlled by the reduced eccentric diagonals (EBF) integrated into the stairs structure, provides higher lateral elastic stiffness, concerning the reference Model A. The behavior factor verifies the highest result: $R = 6.33$.

5.4 | Seismic performance demand

5.4.1 | Models A–B. X-direction

Figure 20a shows that the dissipative members of Model A (compression diagonals) reach the *C* performance level. Figure 20b shows the dissipative members of Model B (some diagonals subjected to compression and tension). The diagonals subjected to compression (left staircase) at elastic range (upper ramps) guarantee the lateral immobility of the stair landing. Knowing that the concentric diagonals in both Models A–B are identical (same length and cross-section), the comparative study under the same seismic demand verified the advantages of relocating the (IV-CBF) diagonals integrated into the stair structure.

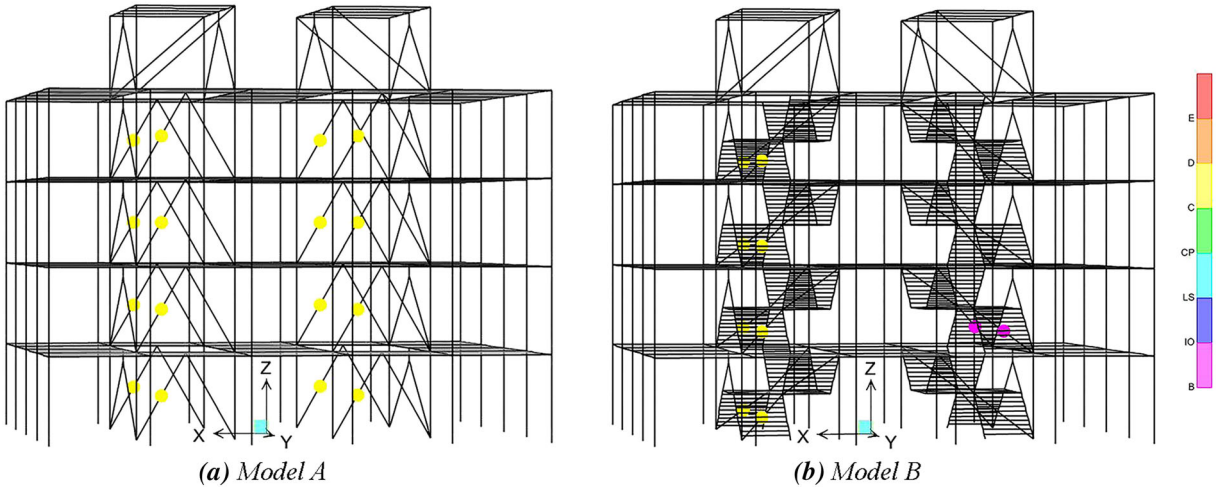

FIGURE 20 Performance levels (seismic demand). Models A–B/Push X

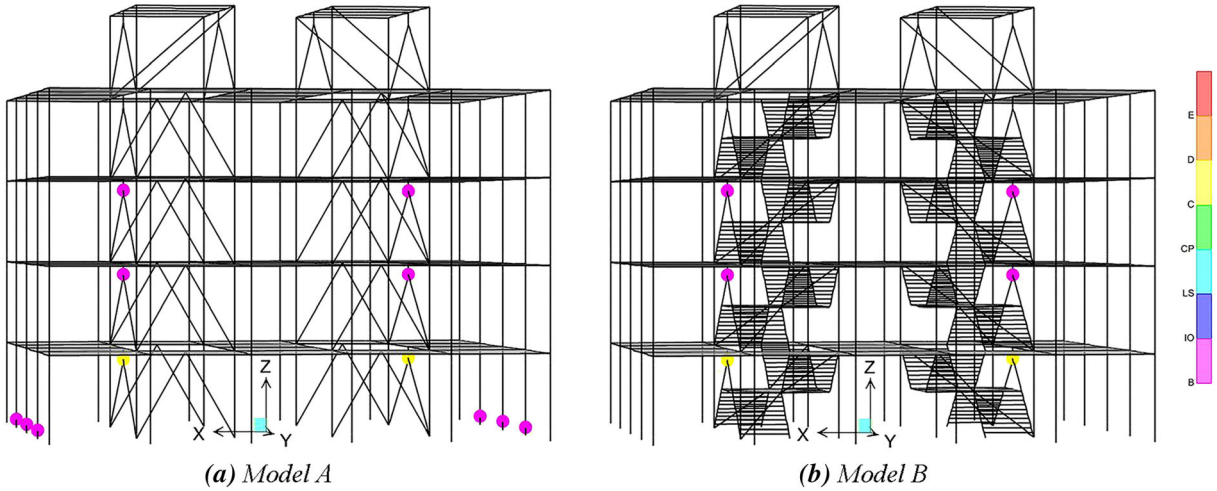

FIGURE 21 Performance levels (seismic demand). Models A-B/push Y

5.4.2 | Models A–B. Y-direction

Figure 21a shows the vertical links and the base columns of Model A that dissipate the seismic energy.

Figure 21b shows Model B with all components of the stairs (rungs and stringers) and the main structure (beams and columns) in the elastic range. The only dissipative members of seismic energy are the replaceable vertical links, verifying the elastic performance in columns, beams, or stairs structures.

5.5 | Seismic performance limitation

Figures 22, 23 show a comparative study according to FEMA 356 limitation of the seismic performance level in the steel members of both Models A–B. The third point defined in each capacity curve (Figure 24) shows the maximum roof displacement regarding the performance level limitation in steel members.

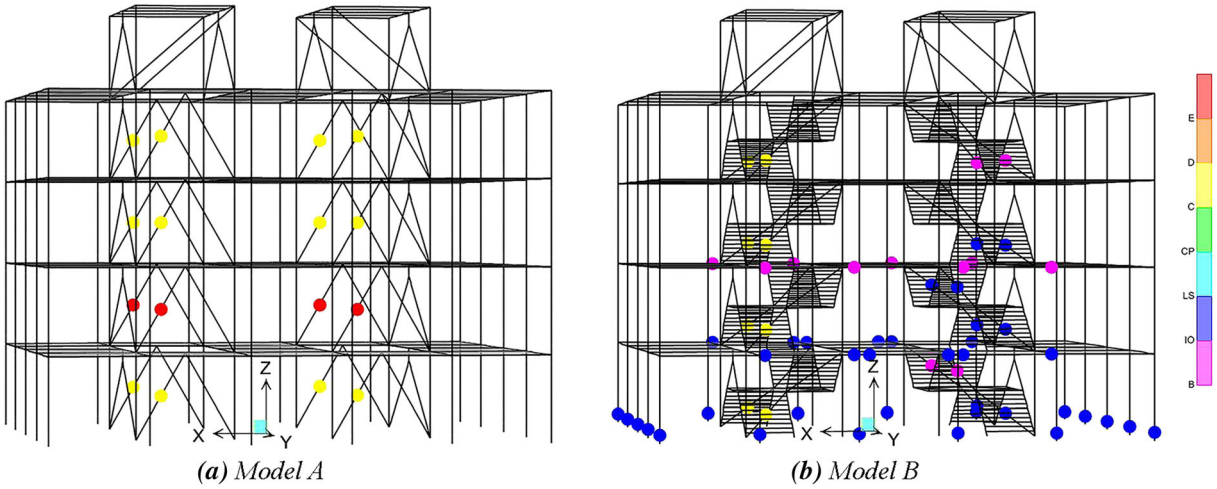

FIGURE 22 Performance level limitation. Models A-B/Push X

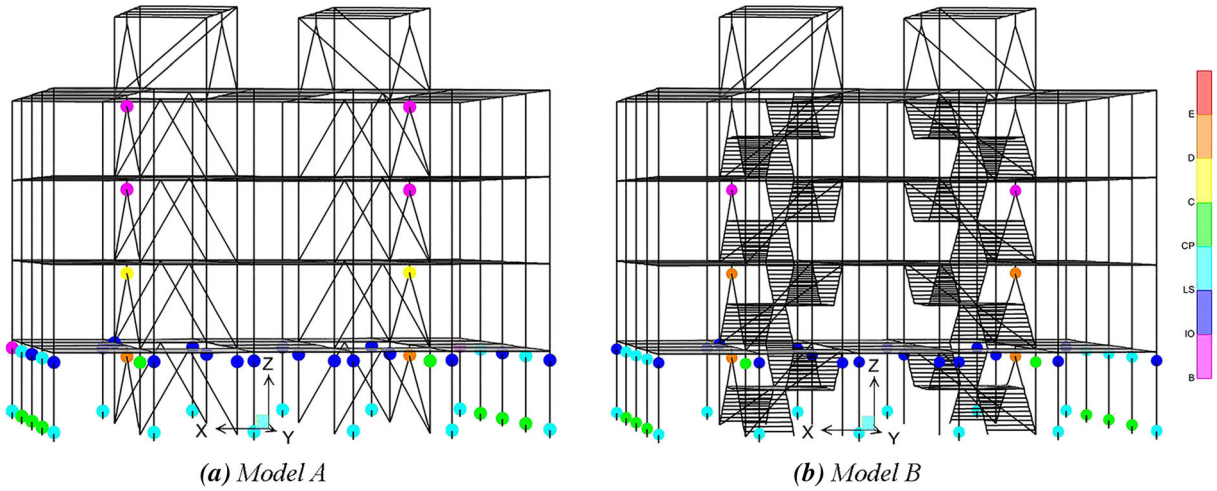

FIGURE 23 Performance level limitation. Models A-B/Push Y

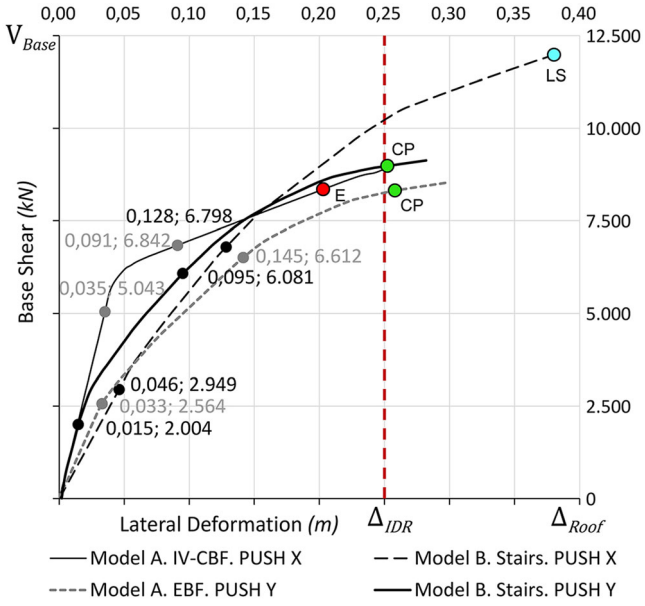

FIGURE 24 Capacity curves. Models A-B/Push X-Y

5.5.1 | Models A–B. X-direction

Figure 22a shows that the drifts of Model A are limited by the buckling collapse of the inverted V-diagonals. Figure 22b shows the seismic performance levels of Model B subjected to the maximum roof drift in the X-direction. The stair stringers and rungs always remain in the elastic range. The upper concentric diagonals (in compression) also remain in the elastic range (controlling the stair landings). The main structure (beams and columns) verifies a high deformation capacity without reaching the *Life Safety* (LS) level.

5.5.2 | Models A–B. Y-direction

Figure 23a shows the Model A limitation by the *Collapse Prevention* (CP) performance level in columns. Figure 23b shows that stair components of Model B remain in the elastic range, guaranteeing structural safety on the evacuation routes. Base columns also show the limitation of the seismic performance (CP) level.

5.6 | Comparative study of capacity curves

This section compares the classical methodology of analysis without stairs (supposedly isolated and capacitated to resist the effects of earthquakes) versus the new approach based on analyzing them as primary elements. Figure 24 shows all capacity curves. Three points were defined on each curve: first, the linear-elastic limit, then the maximum roof displacement according to the seismic demand (ATC-40), and finally, the performance level limitation (FEMA 356). Model A/X-direction curve shows the limit point *E*, caused by the buckling failure of concentric diagonals. Model B/X-direction curve shows the largest roof drift at the *LS* performance level. Both Y-direction curves are limited by the *CP* level (near damage limitation Δ_{IDR}).

Table 14 shows the first two points of each curve (the yield strength point and the performance point) to define the behavior factors. From the first point (yield strength), the elastic stiffness K_{el} is calculated. By multiplying the value of K_{el} by the maximum roof displacement d_{max}, the equivalent linear-elastic force V_E is obtained. Dividing V_E by the base shear in the yield point V_y, the behavior factor *R* is then defined.

TABLE 14 Behavior factors *R*. Models A–B

	A		B	
Model	**X**	**Y**	**X**	**Y**
Roof drift (m)	0.035	0.033	0.046	0.015
Base shear (kN)	5.043	2.564	2.949	2.004
Performance point				
Roof drift (m)	0.091	0.145	0.128	0.095
Eq. elastic shear (kN)	13.112	11.266	8.206	12.692
Behavior factor *R*	2.60	4.48	2.78	6.33

TABLE 15 Comparative seismic analysis. Models A–B

Model **Yield strength point** **Models characteristics**	A		B	
	X	**Y**	**X**	**Y**
Weight (bracings) (kg)	4.864	7.760	4.864	3.232
Elastic stiffness (kN/m)	144.086	77.697	64.109	133.600
Fundamental period (s)		0.696	0.734	
Performance point				
Roof drift (m)	0.091	0.145	0.128	0.095
Behavior factor *R*	2.60	4.48	2.78	6.33

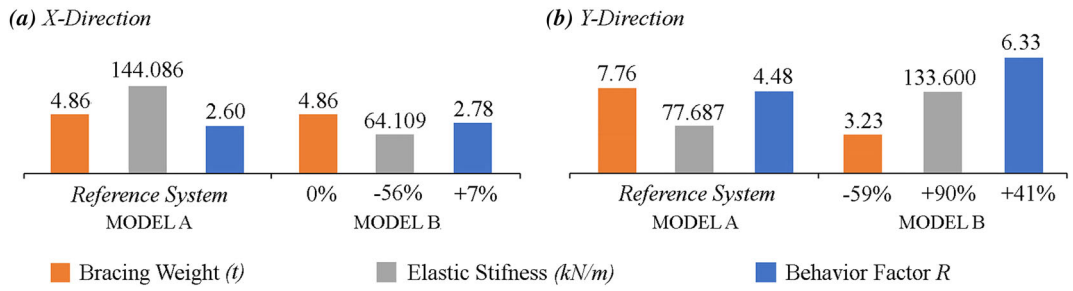

FIGURE 25 Main results of the comparative analysis. Models A–B

5.7 | Summary of comparative analysis

Table 15 presents the results of the preliminary comparative analysis between Models A–B. As shown, when the inverted-V diagonals in 2D frames (Model A) are integrated into the 3D structure of stairs, the X-direction elastic response of the building becomes more flexible. When the long eccentric diagonals in YZ frames are integrated into the stair structure (with a reduced length), the elastic response of the building becomes stiffer.

Figure 25a presents the X-direction comparative analysis. As shown, both models have the same amount of steel in concentric diagonals: W_{A-B} = 4.86 t. However, the typical inverted V-braced frames of Model A verify a higher stiffness (K_{el} = 144.086 kN/m) than Model B (K_{el} = 64.109 kN/m). This low deflection capacity of the typical IV-CBF system causes the danger of buckling failure of diagonals in compression. However, when the same diagonals are integrated into the 3D structure of stairs, the flexibility of the system improves by 56%. The behavior factor of Model A (R = 2.60) agrees with the maximum reference value (R = 2.5) proposed in the seismic standard *(Table 6.2, EC8)* for high ductility class (DCH). Relocating the same diagonals to the stairs, the behavior factor of Model B (R = 2.78) improves by 7%.

Figure 25b shows the Y-direction results. The eccentrical diagonals in Model A require the maximum amount of steel (W_A = 7.76 t) but offer a lower lateral stiffness (K_{el} = 77.687 kN/m). However, by using part of the eccentrical diagonals as stair stringers, the amount of steel is reduced by 59%, and the lateral stiffness of the system is increased. The behavior factor of Model A (R = 4.48) also matches the reference values proposed in EC8 ($R = 4\text{-}5\alpha_u/\alpha_1$) depending on the ductility class (DCM-DCH). The integration of EBFs and stairs increases the lateral stiffness by 90%, improving the behavior factor by 41%. Therefore, Model B/Y-direction verifies the best results of the comparative analysis: The minimum amount of steel in bracings (W_B = 3.23 t), the higher lateral elastic stiffness (K_{el} = 133.600 kN/m), and the maximum behavior factor R = 6.33.

6 | DYNAMIC ANALYSIS OF BRACED STAIRS

6.1 | NLTHA. X-direction

NLTHA of braced stairs considered two design criteria for concentric diagonals[40]:

- Criterion I: *Tension and compression diagonals* (AISC)
- Criterion II: *Only tension diagonals* (EC8)

Figure 26 presents two NLTHA diagrams corresponding to Criterion I (tension and compression diagonals). Figure 26a shows the axial forces in staircases (the rest of the structure is hidden) subject to X-direction loads. All concentric diagonals of the left staircase are in compression, and all those of the right are in tension. Figure 26b shows the building structure mainly braced by diagonals in tension (in elastic range). The upper compression diagonals (CBF2) also brace the stair landings, in the elastic range. The lower diagonals (CBF1) at the C performance level also can contribute to the bracing system of the building.

Figure 27 shows diagrams for the conservative checking of columns and bracings (Criterion II).[41] *IDR* amplification control using tension-rod displacement-restraint bracing[42] may be a new line of research. Figure 27a shows the staircase with only tension (active) diagonals. Compression diagonals are not active. Figure 27b verifies the peak performance level of *Immediate Occupancy* (IO) in tension diagonals (CBF1).

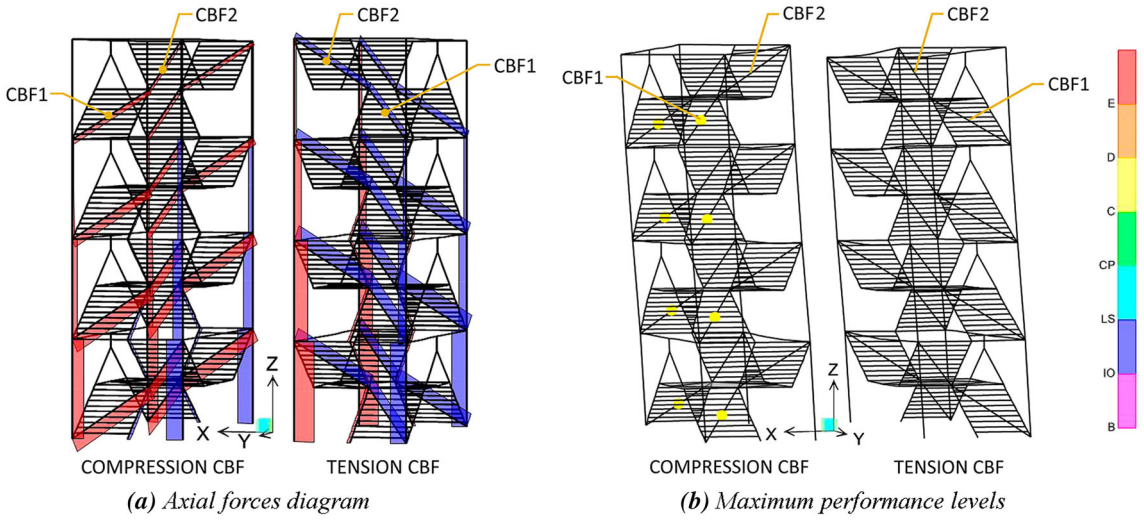

(a) Axial forces diagram *(b) Maximum performance levels*

FIGURE 26 NLTHA-X. Criterion I

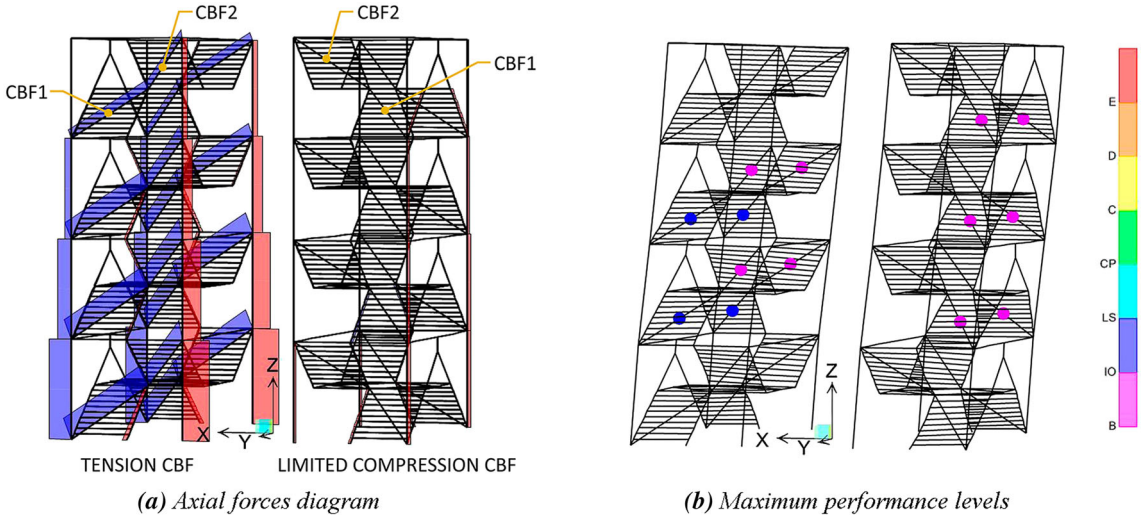

(a) Axial forces diagram *(b) Maximum performance levels*

FIGURE 27 NLTHA-X. Criterion II

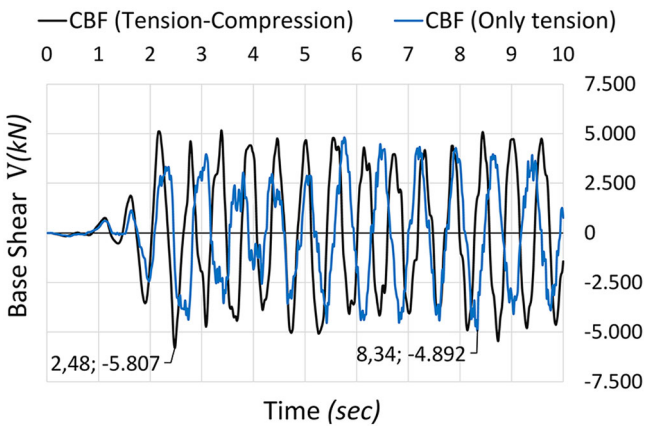

FIGURE 28 NLTHA-X. Criteria I–II. Peak base shear

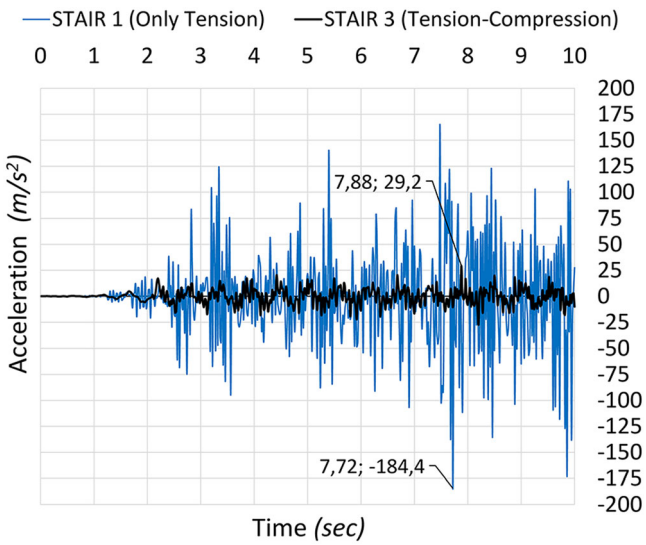

FIGURE 29 NLTHA-X. Criteria I–II. Peak stair acceleration

6.1.1 | Peak base shear

Figure 28 shows the NLTHA diagram of the base shear force according to both Criterion I (tension and compression) and Criterion II (only tension). The peak base shear for Criterion I occurs at t = 2.48 s with a shear force V_b = 5.807 kN. The peak base shear for Criteria II occurs at t = 8.34 s with a shear value V_b = 4.892 kN. These two points determine the approximate time interval of the peaks analyzed below (the maximum inter-story drift and the axial forces in CBF diagonals). Both curves confirm lower base shear values concerning the stronger Y-direction (the X-axis is the direction of the fundamental period of vibration).

6.1.2 | Peak acceleration in stair landings

Figure 29 shows the difference between Criteria I–II, according to the dynamic response of stairs. The NLTHA focuses on the behavior of stair landings, higher acceleration sensitive in the X-direction. The acceleration of the stair landings is increased by inertial forces perpendicular to the stair stringers plane. When the compression forces in diagonals are limited to zero (Criterion II), stairs lack sufficient lateral rigidity against inertial loads. Therefore, the peak acceleration of Stair 1 (only tension) shows inadmissible results (a = 184.4 m/s^2). This effect corresponds to the failure detected in the modal analysis of previous stairs without sufficient lateral rigidity (Figure 13). This diagram confirms the advantages of integrating the concentric diagonals into the stairs structure to control the horizontal inertial forces. The peak acceleration corresponds to Stair 3 (Tension-Compression) at t = 7.88 s with an acceleration value equal to a = 29.2 m/s^2.

6.1.3 | Peak drift between stair landing and floors

The peak roof displacement according to Criterion I (compression and tension) occurs at t = 5.28 s with a roof displacement d = 11.5 cm. According to Criterion II, t = 8.30 s shows the larger drift d = 14.4 cm. The NLTHA focuses on the relative drifts between stairs and floors:

Criterion I. Braced stair landings are correctly kept within the drifts of their two respective floors (Figure 30a).

Criterion II. Stair landings with inactive compression diagonals show larger lateral drifts (Figure 30b).

6.1.4 | Peak axial force and performance level in diagonals (CBF)

Figure 31 shows the axial force diagram of the diagonals in Level III with the higher seismic performance. According to Criterion I, when the compression force in lower CBF1 diagonals reaches the peak performance level C, upper CBF2 diagonals remain in the elastic range (all tension diagonals in the opposite staircase become the main bracing system of the building). According to Criterion II, the peak tension value of lower CBF1 (only tension) diagonals with the higher seismic performance level *IO* is t = 8.64 s, with an axial force N = 1.705 kN.

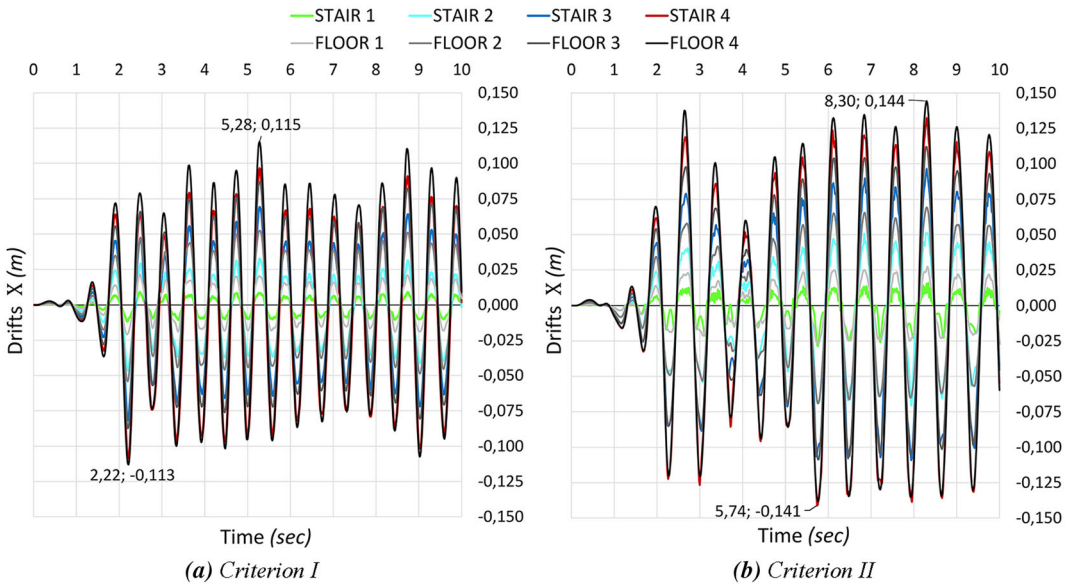

FIGURE 30 NLTHA-X. Stair landings and floor drifts. (a) Criterion I. Braced stair landings are correctly kept within the drifts of their two respective floors. (b) Criterion II. Stair landings with inactive compression diagonals show larger lateral drifts.

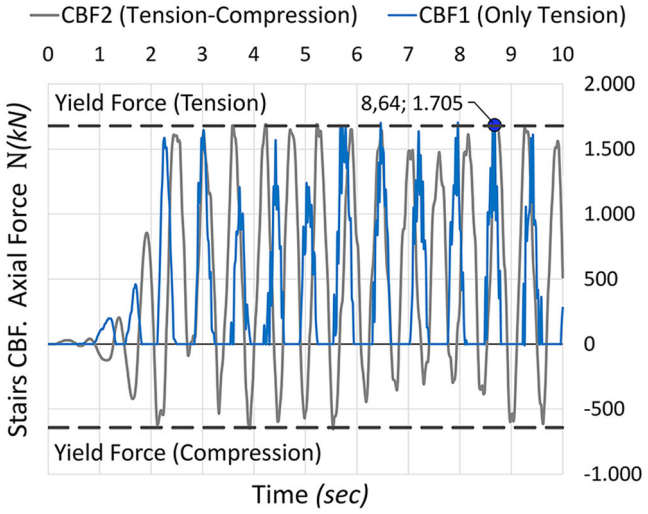

FIGURE 31 NLTHA-X. Peak axial force in concentric diagonals

6.2 | NLTHA. Y-direction

Acceptance criteria for stairs should be based on verification of the ability of the structure to accommodate the inter-story drifts in the Y-direction. Typical stairs are especially deformation sensitive in rigid joints of stringers subjected to inter-story drifts. But the joint releases modeled in the pinned end connections of stair stringers prevent the moment deformation and damage caused by *IDR*. Figure 32 shows the only rigid joint in each story (the union between the vertical link and the eccentric diagonals). Vertical links control the dissipation of seismic energy avoiding damage to stair components. The plastic (hinge) nonlinear rotation θ_p and the shear force V_p in links determine the capacity of the system. Figure 32a shows the bending moments localized only around the single rigid joint of each story. Figure 32b verifies the peak performance level of *Collapse Prevention* (CP) in vertical seismic links.

Figure 33 shows that the dissipation of seismic energy is basically controlled by (easy to repair) vertical links, avoiding structural damage in stairs stringers caused by the relative drifts between floors. According to the seismic performance levels and the deformed shape of the stairs, the satisfactory response is confirmed. Figure 33a shows the NLTHA diagram corresponding to the peak shear force in vertical seismic links. Figure 33b shows the performance levels and maximum deformed shape of the stairs and the main structure.

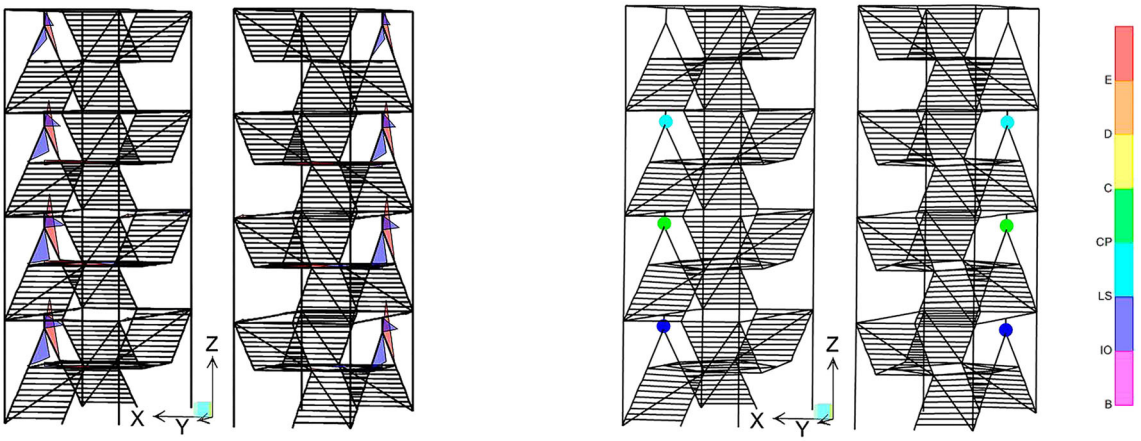

(a) Moment diagram *(b) Maximum performance levels*

FIGURE 32 NLTHA-Y. 3D view

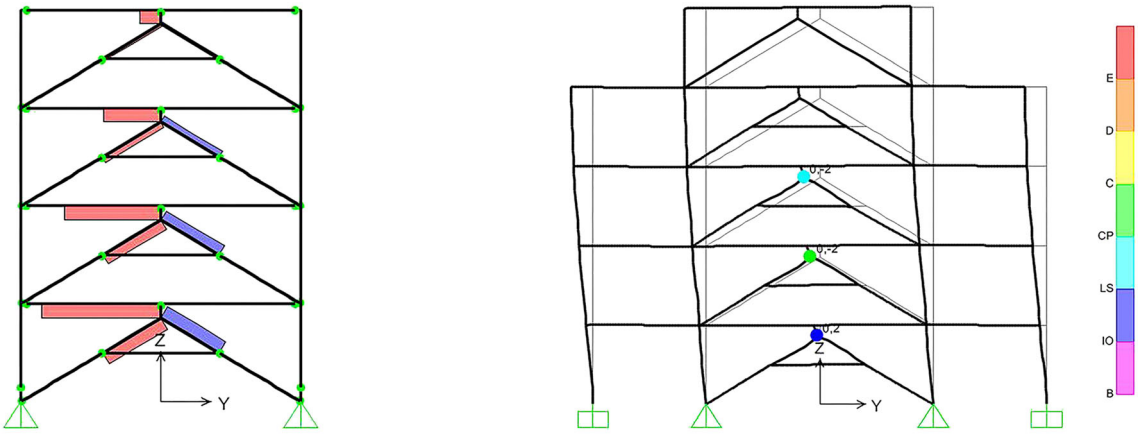

(a) Shear forces diagram *(b) Deformed and performance levels*

FIGURE 33 NLTHA-Y. 2D view

6.2.1 | Peak base shear

Figure 34a shows the peak base shear at time interval t = 4.56 s with the value V_b = 7.901 kN. The higher values of base shear force in the Y-direction confirm the X-direction as the fundamental period of vibration.

6.2.2 | Peak acceleration in stair landings and floors

Figure 34b *Peak horizontal floor acceleration* (PHFA) is used for estimating the vulnerability of acceleration-sensitive nonstructural elements. This *NLTHA* diagram confirms that the last Stair Landing 4 is well coupled to the dynamic response of Floor 4 (time t = 4.72 s with a value $a = 19.39\ m/s^2$).

6.2.3 | Peak drift between stair landing and floors

Figure 35 shows the NLTHA-Y-direction drifts of stair landings and floors. The peak drift in Stair 2 (Link 2) causes a higher seismic performance level *CP*. The time value of the largest displacement is t = 4.76 s defined by the displacement of Floor 1 (d = 1.6 cm) and Floor 2 (d = 3.2 cm).

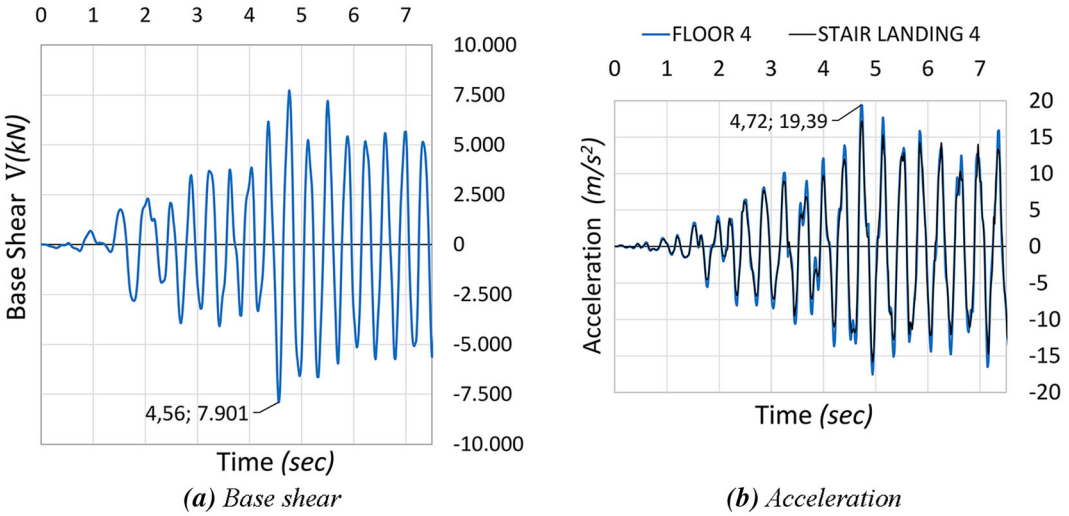

FIGURE 34 NLTHA-Y

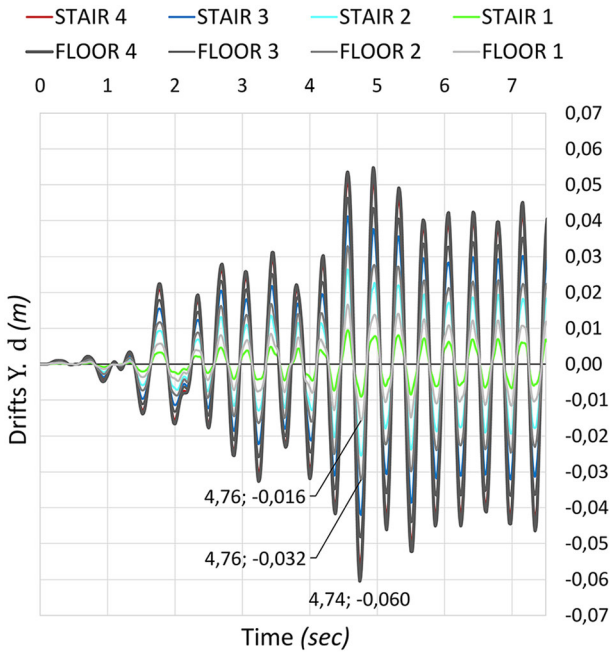

FIGURE 35 NLTHA-Y. Stair landings and floors drifts

6.2.4 | Peak plastic (hinge) nonlinear rotation (EBF)

Figure 36 shows the plastic (hinge) nonlinear rotation of the rigid joint between the eccentric diagonals and links. The nonlinear rotation θ_p in links should be limited ($\theta_p \leq 0{,}08$ rad) according to *6.8.2* [10], *EC8*. The peak rotation (Link 3) at the time interval t = 4.74 s show the value $\theta_p = 0{,}013$ rad < 0,08 rad. These satisfactory results also confirm the low deformation of the braced stair system (Figure 33b).

6.2.5 | Peak shear force and performance level in links (EBF)

Figure 37 shows the NLTHA shear force diagram corresponding to the vertical Link 2 with the higher seismic performance level *(CP)*. The time at the peak shear force occurs at t = 4.76 s with the value V = 2.362 kN. The stairs structure subjected to the El Centro accelerogram verifies satisfactory results.

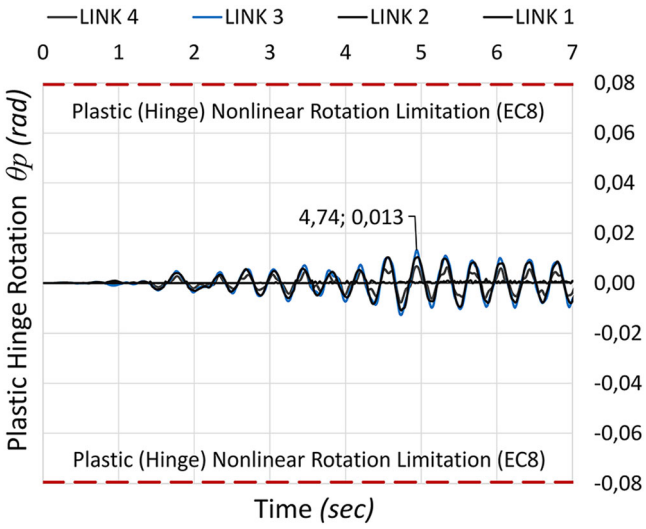

FIGURE 36 NLTHA-Y. Plastic (hinge) nonlinear rotation θ_p in (EBFs) links

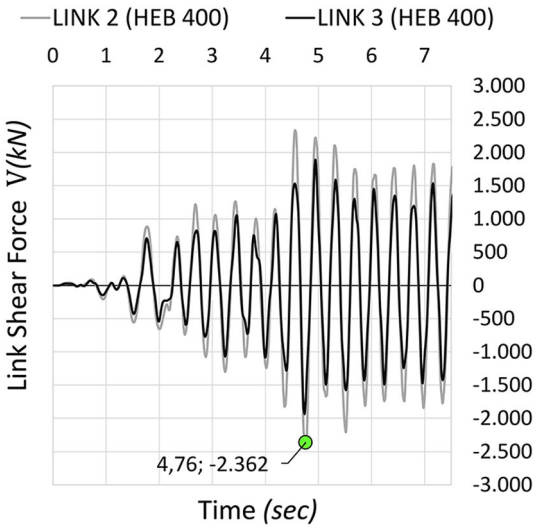

FIGURE 37 NLTHA-Y. Shear forces in vertical links (EBFs)

6.3 | Summary of Dynamic analysis

Table 16 presents the X-direction results. Two methodologies of analysis estimate the nonlinear cyclic behavior of the concentric diagonals: Criterion I *(tension and compression)* and Criterion II *(only tension)*. The peak base shear according to both Criteria I–II (V_b = 4.892–5.807 kN) verifies lower values concerning the Y-direction (V_b = 7.901 kN). The peak acceleration according to Criterion I confirms that stairs landings are well braced by concentric diagonals (a = 29.2 m/s^2). However, Criterion II is not useful for the analysis of stair landing acceleration (a = 184.4 m/s^2) because of the hypothesis that all compression diagonals are inactive. The peaks roof drifts according to both Criteria I–II verify the values d_{Roof} = 11.5–14.4 cm. However, the main difference is the local response of stair landings: centered concerning the *IDR* (Criterion I) or larger (Criterion II). Criterion I is useful to verify the maximum seismic performance level C in lower compression diagonals. Criterion II is used to estimate the maximum axial force on columns and the tension force in diagonals with the highest performance level (Stairs 3/CBF1, N = 1.705 kN). Table 17 presents the Y-direction results. All the seismic performance is concentrated only in vertical links, whose peak plastic (hinge) nonlinear rotation complies with the EC8 provisions (θ_p = 0,013 rad < 0,08 rad), and their peak shear force (V = 2.362 kN) verifies the satisfactory performance level CP. Figure 38 presents the decisive verification (Section 3.3 *Design rules for steel bracings*) of damage limitation according to maximum *IDR (4.4.3.2, EC8)*, most unfavorable concentric diagonals (Criteria I–II), and links.

TABLE 16 NLTHA. X-direction

Criteria	I		II	
Interval	**T (sec)**		**T (sec)**	
Peak base shear		**V (kN)**		**V (kN)**
	2.48	5.807	8.34	4.892
Peak acceleration		**a (m/s^2)**		**a (m/s^2)**
Stair Landing 2	7.88	29.2	(9.70)	(127.7)
Floor 4	8.72	16.8		
Peak floors-stair drift		**d (m)**		**d (m)**
Floor 3	2.22	0.087		
Stair Landing 3	2.22	0.082		
Floor 2	2.22	0.054		
Relative drift (Levels 2–3)		0.033		
Peak axial force/perform. level		**N (kN)**		**N (kN)**
Stair 3/CBF1 (only tension)			8.64	1.705
Stair 3/CBF2 (compression)		−651.7		

TABLE 17 NLTHA. Y-direction

Interval		
Peak base shear	**T (sec)**	**V (kN)**
	4.56	7.901
Peak acceleration		**a (m/s^2)**
Stair Landing 4	4.70	19.4
Floor 4	4.70	15.4
Peak floors-stair drift		**d (m)**
Floor 2	4.76	0.032
Stair Landing 2	4.76	0.025
Floor 1	4.76	0.016
Relative Drift (Levels 1–2)		0.016
Peak plastic (hinge) rotation		**θ_p (rad)**
Link 2	4.74	0.013
Peak (link) shear force/Perform. level		**V (kN)**
Link 2	4.76	2.362

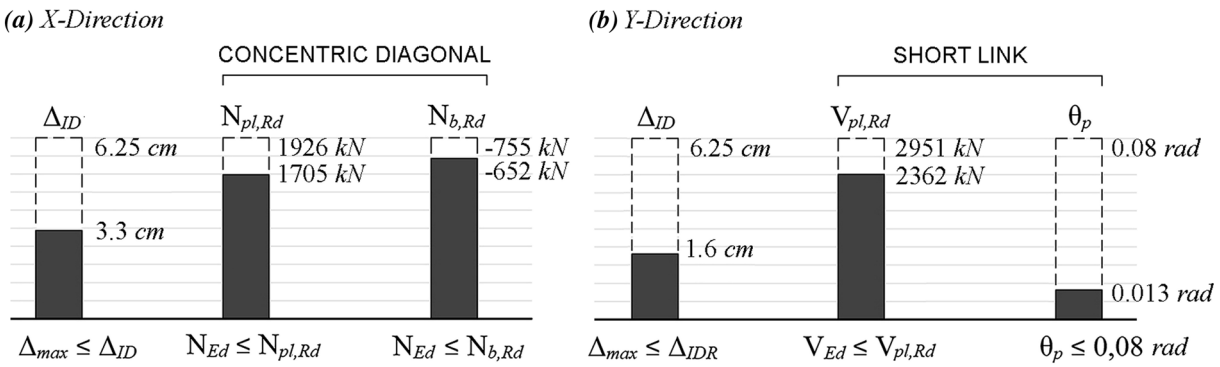

FIGURE 38 Main results of stairs bracing members with maximum performance level

7 | CONCLUSIONS

This paper presents a new line of research focused on the typological and structural design of stairs as primary elements of steel buildings.[43] The research proposes a novel approach to the architectural project, structural design, and seismic analysis of steel buildings with stairways. The analysis methodology focuses on the structural safety of escape routes and their favorable effect on building behavior. Given the satisfactory results obtained in the comparative and dynamic analyses, the following conclusions should motivate further research and experimental tests on braced stair systems:

- Architectural issues caused by bracing diagonals are solved by integrating them into the stair structure.
- The braced stairs improve the structural safety of escape routes and their effect on building behavior.
- Unmodeled/isolated stairs waste their contribution to the lateral force resistance system of buildings.
- The amount of steel in the reference eccentric diagonals was reduced in the braced stair system by 59%.
- Easily repairable steel members (CBF-EBF) can dissipate the seismic energy avoiding damage to stairs.
- The special braced stairs improved the R_x behavior factor of the typical IV-CBF system by 7%.
- The integration of the EBF system into the stairs increased the seismic behavior factor R_y by 41%.
- The (X-direction) acceleration in stair landings braced by concentric diagonals was reduced by 75%.
- Damage in stairs stringers is avoided by pinned end connections and eccentric bracing (EBFs).
- The deterministic analysis of braced stairs verified satisfactory results compared to the reference systems.
- Results motivate further research (new designs, analysis, and experimental tests) on braced stair systems.

CONFLICT OF INTEREST

The authors declare no competing financial interests or personal relationships that have influenced the article.

DATA AVAILABILITY STATEMENT

Research data are not shared.

ORCID

Carlos Montalbán Turon https://orcid.org/0000-0003-2275-8560

REFERENCES

[1] S. Lay, *Struct. Des. Tall Spec. Build* **2007**, *16*, 487. https://doi.org/10.1002/tal.412
[2] South Carolina Geological Survey, SCGS, Columbia, EUA **2022**. https://www.dnr.sc.gov/geology/earthquake-info.html
[3] D. Bull Stairs & access ramps between floors in buildings. Canterbury Earthq. Royal Commission, New Zealand **2011**.
[4] H. Sun, A. Zhang, J. Cao, *Eng. Fail. Anal.* **2013**, *33*, 490. https://doi.org/10.1016/j.engfailanal.2013.06.023
[5] I. A. Tegos, V. P. Panoskaltsis, S. D. Tegou, in *4th ECCOMAS*, (Eds: M. Papadrakakis, V. Papadopoulos, V. Plevris), COMPDYN 2013, Kos Island, Greece **2013** 3259 10.7712/120113.4736.C1745.
[6] Z. Cao, C. Bian, C. Xu, in *ICMCE*, (Eds: W. Z. Chen, X. Wu, J. Xu), Atlantis Press, Shenyang, China **2014** 478 10.2991/icmce-14.2014.82.
[7] C. Higgins, *J Struct Eng* **2009**, ASCE, *135*(2), 122. https://doi.org/10.1061/(ASCE)0733-9445(2009)135:2(122)
[8] X. Wang, R. Astroza, T. Hutchinson, J. P. Conte, J. I. Restrepo, *Earthq. Eng. Struct. Dynam.* **2015**, *44*(14), 2507. https://doi.org/10.1002/eqe.2595
[9] C. J. Black, I. D. Aiken, K. W. Smith, R. J. Belvin, A. J. Peachey, Seismically-resilient stair systems for buildings. *In the Proceedings of the Structural Engineers Association Annual Convention. Paper #22*. San Diego, California **2017**.
[10] X. Wang, T. C. Hutchinson, *Eng. Struct.* **2018**, *166*, 376. https://doi.org/10.1016/j.engstruct.2018.03.074
[11] C. Xu, T. Li, in *EMEIT-2012*, Atlantis Press, Paris, France **2012**. https://doi.org/10.2991/emeit.2012.91
[12] H. J. Jiang, H. Y. Gao, B. Wang, *Adv. Mat. Res.* **2012**, *446*, 2326. https://doi.org/10.4028/www.scientific.net%2FAMR.446-449.2326
[13] F. U. H. Mir, D. Rai, *Earthq. Eng. Struct. Dynam.* **2020**, *49*(6), 527. https://doi.org/10.1002/eqe.3251
[14] Y. Feng, X. Wu, Y. Xiong, C. Li, W. Yang, *Earthq. Eng. Eng. Vib.* **2013**, *12*, 209. https://doi.org/10.1007/s11803-013-0164-2
[15] A. Noorifard, M. Tabeshpour, *Arch. Civ. Eng. Env.* **2018**, *11*(4), 105. https://doi.org/10.21307/ACEE-2018-058
[16] Y. Zhang, P. Tan, H. Ma, M. Donà, *Comp. Mod. Eng. & Scie.* **2020**, *124*(2), 415. https://www.techscience.com/CMES/v124n2/39530
[17] Applied Technology Council, ATC-40, Washington D.C., EUA **1995**.
[18] Federal Emergency Management Agency, FEMA 356, Washington DC, EUA **2000**.
[19] European Committee for Standardization, *EC8(part 1) UNE-EN 1998–1:2018*, CEN, Brussels, Belgium **2004**.
[20] Federal Emergency Management Agency, FEMA P-750, Washington DC, EUA **2009**.
[21] Federal Emergency Management Agency, FEMA E-74, Washington DC, EUA **2012**.
[22] American Society of Civil Engineers, ASCE/SEI 7-10, EUA **2010**.
[23] American Society of Civil Engineers, *ASCE/SEI 41-06*, EUA **2007**.
[24] F. Clementi, E. Quagliarini, G. Maracchini, S. Lenci, *Jour. Build. Eng.* **2015**, *4*, 152. https://doi.org/10.1016/j.jobe.2015.09.008
[25] Singapore Civil Defense Force Government Agency, *Code of Practice for Fire Precautions in Buildings*, Singapore Civil Defense Force (SCDF), Singapore **2018**.

[26] European Committee for Standardization, EC3(Part 1) UNE-EN 1993:1–1:2013, CEN, Brussels, Belgium **2013**.
[27] H. Degée, A. Plumier, *Eurocode 8: Seismic Design of Buildings Worked Examples*, JRC, Ispra, Italy **2012**.
[28] Federal Emergency Management Agency, FEMA 350, Washington DC, EUA **2000**.
[29] R. Montuori, E. Nastri, V. Piluso, *Jour. Const. Ste. Res.* **2014**, *92*, 122. https://doi.org/10.1016/j.jcsr.2013.10.009
[30] M. Lian, M. Su, *Struct. Des. Tall Spec. Build.* **2018**, *27*(5), 1455. https://doi.org/10.1002/tal.1455
[31] A. Ghamari, M. Vetr, *Build.* **2019**, *28*(11), 1587. https://doi.org/10.1002/tal.1587
[32] L. Shen, Q. Wang, X. Li, J. Tian, *Struct. Des. Tall Spec. Build.* **2019**, *29*(11), 1689. https://doi.org/10.1002/tal.1689
[33] M. Fahiminia, M. R. Ghaderi, S. M. Zahrain, *Struct. Des. Tall Spec. Build.* **2019**, *28*, 14. https://doi.org/10.1002/tal.1658
[34] Computers and Structures Inc, SAP2000, Berkeley, EUA **2010**.
[35] E. Cosenza, G. M. Verderame, A. Zambrano, *14th WCEE*, Beijing, China **2008**.
[36] J. Magdy, Z. Khalil, M. Elsarag, M. Darwish, in *International Congress and Exhibition SCI*, (Eds: H. Rodrigues, A. Elnashai, G. Calvi), Springer Cham, New York **2017** 83 10.1007/978-3-319-61914-9_7.
[37] Federal Emergency Management Agency, *FEMA 440*, EUA, Washington DC **2005**.
[38] R. L. Mayes, *Struct. Des. Tall Spec Build.* **1995**, *4*(1), 15. https://doi.org/10.1002/tal.4320040104
[39] J. Goggins, S. Salawdeh, *Earthq. Eng. Struct. Dynam.* **2013**, *42*(8), 1151. https://doi.org/10.1002/eqe.2264
[40] S. K. Azad, C. Topkaya, A. Astaneh-Asl, *Jour. Const. Ste. Res.* **2017**, *133*, 383. https://doi.org/10.1016/j.jcsr.2017.02.026
[41] A. Di Cuia, L. Lombardi, F. De Luca, R. De Risi, S. Caprili, W. Salvatore, *Proc. Eng.* **2017**, *199*, 3522. https://doi.org/10.1016/j.proeng.2017.09.502
[42] H. Tagawa, K. Inooka, *Struct. Des. Tall Spec Build.* **2018**, *27*(2), 1411. https://doi.org/10.1002/tal.1411
[43] C. Montalbán, in Ph.D. theses: *Structural analysis of stairs for buildings against wind and earthquakes*. Director: Robert Brufau Niubó. Ponent: Ramon González Drigo, Dep. Civil & Env. Eng., (DECA), UPC, Barcelona, Spain 2021. https://futur.upc.edu/31929491

How to cite this article: C. Montalbán Turon, Y. F. Vargas Alzate, *Struct Design Tall Spec Build* **2023**, e1997. https://doi.org/10.1002/tal.1997

APPENDIX A

TABLE A1 Seismic standard criteria for the structural design of special braced stairs

Code	ATC	EC	FEMA		
Document	40	8	356	P-750	E-74
Seismic standard criteria					
The collapse of *stairs* is a risk for people and must be verified, under seismic action.	X	X	X	X	X
Stairs may be independent or integral to the main structure.	X		X		X
If *stairs* influence the lateral force-resisting system may be considered primary elements.	X	X	X		X
Primary elements must be modeled and designed for seismic resistance.	X	X	X	X	X
Stairs are primary elements if exceed 15% of the lateral stiffness of the main structure.		X			
Stairs may take the form of structural reinforcement.			X		
Stair acceptance criteria should consider gravity loads, seismic forces, and IDR.		X	X		X
Emergency stairs should be usable at Life Safety seismic performance level.			X		
Performance level Collapse Prevention poses a risk due to the failure of stairs.			X		
Stairs should not change the building classification from non-regular to regular.	X	X	X		
Damage limitation according to inter-story drifts and *stairs* ductility should be verified.		X		X	X
The main structural safety problem in stairs is the IDR due to lateral seismic loads.		X		X	
Stairs attached to adjacent frames or floors are sensitive to deformations.					X
Unfixed and unbraced stair landings are sensitive to acceleration and inertial loads.					X
Bracing and restrictive IDR limitations serve to control the damage.		X		X	
Stair components (e.g., rungs) can be damaged if they are not provided with strength.					X
Stairs without ductile connections can suffer serious damage.			X	X	X
Acceptance criteria focus on strength of stairs to resist out-of-plane forces and IDR.			X		X